Techno-economic assessment of biogas-fed CHP hybrid systems in a real wastewater treatment plant

Energy Modelling and Techno-economic Analysis of a Biogas-fed CHP SOFC System Integrated with Microturbine: Case Study for a Wastewater Treatment Plant

M. MosayebNezhad[1], A. S. Mehr[2*], M. Gandiglio[1], A. Lanzini[1], M. Santarelli[1]

1. Department of Energy, Politecnico di Torino, Turin, Italy
2. Department of Mechanical Engineering, University of Tabriz, Tabriz, Iran

Abstract

Wastewater Treatment Plants (WWTP) have a significant role in both processing wastewater to return to the water cycle, and in transforming between 40% and 60% of the dissolved organic matter into a non-fossil combustible gas (biogas) with a methane content of around 50–70 vol. %. Combined heat and power (CHP) concepts for small-scale distributed power generation offer a significant potential for saving energy and reducing CO_2 emissions. In this paper, an integrated configuration of an SOFC system and a Microturbine (MGT) in a reference WWTP is proposed. The concept is to utilize the available biogas in the plant to feed the SOFC and MGT to not only produce electrical power but also to provide the digester thermal demand. For the sake of comparison, the base case (SOFC is the only CHP unit) and the MGT case (integration of SOFC and microturbine systems) are proposed. Four additional scenarios using the performance of commercial micro turbines are developed varying both the size and the operating mode (constant vs. modulating power output). Results show that the use of the MGT along with the SOFC can increase the share of electricity covered by self-generation within the WWTP, while keeping stable the coverage of the thermal load. From an economic point of view, with short and long term cost scenarios for the SOFC system, the best configuration is the one related to an SOFC integrated with a small MGT installation working with partial load operation.

Keywords: *Solid Oxide Fuel Cell, microturbine, CHP, wastewater treatment plant, biogas, economic analysis.*

***Corresponding author:** Dr. Ali Saberi Mehr
Email address: A.S.Mehr@tabrizu.ac.ir (ali.saberi07@gmail.com)

1. Introduction

The “Europe 2020” strategy promotes the shift towards a resource-efficient, low-carbon economy to achieve sustainable growth. The European policies on energy and sustainability are thus contributing to the diversification of the primary energy sources and to the introduction of distributed power technologies with high efficiency and low carbon emissions (European Strategic Energy Technology (SET) Plan for 2020 [1]).

One of the technologies playing a key role in achieving the goals of the mentioned strategy and has been paid much attention in recent years is the Fuel Cell technology. Solid oxide fuel cell (SOFC) is an interesting choice as like most fuel cell technologies have some advantages such as being modular, scalable, and efficient. Compared to other fuel cells, the SOFCs are fuel-flexible and can reform methane internally, use carbon monoxide as a fuel, and tolerate some degree of common fossil fuel impurities, such as ammonia and chlorides [2]. On the other hand, microturbine technology is an almost well-known and commercially developed for small scale power production. In his context, the integration of SOFC and microturbine systems has been of great interest for research to develop new hybrid systems which offer higher efficiency.

1.1 Literature review

Williams et al. [3] proposed an indirect SOFC-GT hybrid system. They reported that the maximum achievable efficiency for their system is 45%. Also, it is shown that their system has lower efficiency value than that of the direct combination of the two systems. Cheddie et al. [4] proposed an indirect combination of an SOFC system into a 10 MW gas turbine plant. According to the developed thermo-economic model, it was predicted that under the optimized condition the system could produce 20.6 MW power with an efficiency of 49.9%. In another research [5], a semi-direct integration of an SOFC and a gas turbine was studied. Thermo-economic optimization results revealed that for the studied system, an output power of 21.6

MW could be obtained with an efficiency of 49.2%. Zhang et al. [6] proposed a new model for an SOFC- GT system. In their work, the waste heat from SOFC stack as well as the combustion chamber is utilized to heat up the gas turbine inlet. It is claimed that the hydrocarbons are feasible fuels for the SOFC. Bicer and Dincer [7] proposed a scheme consisting of a steam-assisted gravity drainage, underground coal gasification, solid oxide fuel cell, integrated gasification combined cycle and an electrolyzer. Energy and exergy efficiencies of 19.6% and 17.3% are obtained for the combined system, respectively. Zhao et al. [8] studied a coal syngas fueled SOFC stack working in an atmospheric condition which is indirectly integrated into a Brayton cycle. is the authors concluded that the system efficiency increases with decreasing current density and the value could be in a range of 48-56%, depending on the operating temperature and current density. Inui et al. [9] introduced two types of carbon dioxide recovering SOFC-GT combined power generation systems in which a gas turbine either with carbon dioxide recycle or with water vapor injection is adopted as the bottoming cycle. Reportedly, with carbon dioxide recycle the overall efficiency of 63.87% (HHV) or 70.88% (LHV) is reached. These values for the system with water vapor injection are 65.00% (HHV) or 72.13% (LHV), respectively. Eveloy et al. [10] investigated an indirect combination of a gas turbine with an internal reforming SOFC system and an organic Rankine cycle (ORC) thermodynamically and economically. For toluene as the ORC working fluid, it is stated that the SOFC-GT-ORC system demonstrates an efficiency improvement of about 34% compared to the gas turbine as a stand-alone system, and of 6% compared to the hybrid SOFC-GT sub-system. It is predicted that the system would become profitable within three to six years. Inui et al. [11] proposed a combination of SOFC and closed cycle magneto hydrodynamic (MHD)/noble gas turbine with carbon dioxide recovery. It is reported that the overall thermal efficiency of the system using methane as the fuel could be 63.66% (HHV) or 70.64% (LHV). Sànchez et al. [12] compared the performance of conventional regenerative gas turbine with

the direct/indirect integration of the SOFC and GT systems at full and part loads. is the authors concluded that the indirect hybrid system is less efficient than the direct one since power and efficiency enhancement caused by the higher pressure in the SOFC is not present in the indirect system. It is also found that the total cost of a fuel-cell-based configuration is lower despite the greater initial investment/installation cost of an integrated system. Bin Basrawi et al. [13] investigated the performances of a biogas-fuelled micro gas turbine cogeneration system in different scales of sewage treatment plants for various output powers under various ambient temperature conditions.

1.2 Present work

In the most of the previous researches regarding the integration of gas turbine and SOFC system, the process of the production of fuels to feed the SOFC has not been considered. In addition, integration of gas turbine and SOFC systems normally requires high-pressure system. In this article, a new combination of SOFC and micro gas turbine technologies in atmospheric pressure level for a wastewater treatment plant is proposed. A multi-scale simulation is performed involving both the detailed simulation of the SOFC and MGT system considering the biogas production process as well as the thermal integration of the whole wastewater treatment plant on a larger scale. The present research is a part of EU project called DEMOSOFC [14] which is a Fuel Cell & Hydrogen Joint Undertaking (FCH2-JU) funded project foreseeing the installation of the largest (in 2016) biogas fed Solid Oxide Fuel Cell (SOFC) in Europe.

1.3 DEMOSOFC Project

The SOFC will be the sole combined heat & power (CHP) generator within a medium-size wastewater treatment plant (WWTP) located in Torino (IT) (Figure 15). The mentioned

reference WWTP serves 270'000 equivalent inhabitants collecting an overall of 59'000 m^3 of wastewater on a daily basis that corresponds to ~220 liter/day/capita [15].

The objectives of this project can be summarized as follows:

1. Demonstration and detailed analysis of an innovative solution of distributed sub-MW CHP system based on SOFC, with high interest in the industrial/commercial application.
2. Demonstration of a distributed CHP system fed by biogas from anaerobic digestion
3. Demonstration of the high performance of such systems: electrical efficiency, thermal recovery, low emissions, plant integration, economic interest
4. Exploitation and business analysis of this type of innovative energy systems
5. Dissemination of the high interest (energy and economic) of such systems

Figure 1. SMAT wastewater treatment plant in Collegno (Turin) [16]. "DEMOSOFC Plant" shows the area where the three SOFC modules will be installed.

The main concept of the DEMOSOFC project is illustrated in **Errore. L'origine riferimento non è stata trovata.**. The DEMOSOFC plant comprises the following sections [14]:

1. Biogas processing unit: The unit includes biogas dehumidification, contaminants removal and compression. Biogas from Collegno WWTP still contains hydrogen sulfide and siloxanes, both harmful for the fuel cell. These contaminants are removed via an adsorption-based system that uses activated carbons. Before the clean-up system, biogas is cooled and water is removed in a chiller, in order to guarantee the carbon optimal operation parameters. A gas analyzer, able to detect both H_2S and siloxanes, is installed to online measure macro-composition and contaminants concentration both at the inlet and outlet of the clean-up system.

2. SOFC modules: The system is composed of 3 modules, able to produce about 58 kW AC each so the total amount of installed power is around 174 kWe.
3. Heat recovery system: Hot exhaust from the SOFC modules heats a water loop, able to provide partial heating to the sludge entering the digester. A new heat recovery loop is integrated with an existing one, where heat is provided by a boiler fed by extra biogas or natural gas from the grid.
4. A general control system is also implemented in order to control the system, both on site and remotely.

In the present research, the premise of the effort is to modify the current configuration of the DEMOSOFC project using the microturbine along with SOFC systems. In the following, a brief technology overview of two key components (SOFC and microturbine prime movers) of the plant is presented.

Figure 2. Concept diagram of the DEMOSOFC plant [14].

2. Description of the technology

2.1 SOFC system configuration

Figure 3a illustrates the proposed SOFC system layout in the plant. Air (state 1) is pre-heated in the air heat exchanger after being pressurized through the air blower (state 2). Then it is sent to the cathode side of the stack (state 3). Clean fuel (biogas/NG) is pressurized using the fuel blower before mixing with the anode gas recycle. The mixed gas is sent to the pre-reformer (state 6) where a fraction of methane is converted to hydrogen and carbon monoxide through reforming and shifting reactions. The reformer is modeled as an adiabatic reactor, where outlet temperature (state 7) and methane conversion are calculated depending on the inlet conditions. No external heat is thus required in this configuration. Then, the reformed gas is pre-heated through the fuel heat exchanger before feeding the anode side of the stack (state 8). The fuel gas experiences an internal reforming which brings a hydrogen-rich mixture participating in

160 the electrochemical reaction inside the fuel cell stack. Internal reforming has been considered
161 as IIR (Indirect Internal Reforming), thus taking place not directly on the anode catalyst but on
162 a physically separated catalyst thermally connected to the fuel cell in order to receive the
163 required heat for the reaction. The electrochemical reaction generates thermal energy, a part of
164 which is used to deliver the required heat for the internal reforming reaction, another part is
165 employed to heat up the cell products and the residual reactants.
166 Anode and cathode exhaust gases (state 9 and state 4) with higher temperatures are obtained
167 and electrical power is produced. An inverter is used to convert the DC power generated by the
168 stack into AC grid-quality electricity. After accomplishing the electrochemical reactions in the
169 SOFC, the excess air exiting the cathode (state 4) and the unreacted fuel exiting the anode (state
170 12) are supposed to combust completely in the after-burner. However, a fraction of anode exit
171 gas (state 11) is recirculated back to the mixer to be mixed with the fuel. A given amount of
172 Steam-to-Carbon (SC) ratio, to avoid using external demineralized water, is defined for which
173 the amount of recirculation fraction would be calculated. The exhaust stream of the SOFC units
174 is sent to the exhaust heat recovery exchanger which will be explained in detail in the following
175 sections.
176 Figure 3a. Proposed SOFC system layout.

177 **2.2 Micro gas turbine (MGT) technology**

178 MGTs can be defined as small, compact high-speed turbo-generators of between 30 and 300
179 kW_e that can deliver energy in the form of electricity and heat [17]. Basically, MGTs are based
180 on a Brayton cycle and usually consist of a centrifugal compressor, a radial turbine and a
181 permanent magnet alternator rotor. Their main features are that the high-speed generator is
182 directly coupled to the turbine rotor and that they use power electronics instead of a gearbox
183 and conventional generator to adapt the power produced to the grid power quality.

184 The microturbine efficiency can increase by taking advantage of regeneration and is meant to
185 pre-heat the air at the burner inlet by exploiting the hot gases exhausted from the turbine as can
186 be seen in Figure 3b.

187 Figure 3b Schematic of the regenerated microturbine system

188 # 3. Integrated cogeneration system

189

190 As discussed there is a potential of utilizing the available biogas in the SMAT Collegno to
191 produce electrical power. Considering the use of SOFC to produce power as a base scenario
192 which is supposed to be performed in DEMOSOFC project, base case layout is defined. In this
193 case, the available biogas is just to be used in the SOFC units, meanwhile SOFC exhaust
194 thermal energy as well as a boiler are used to supply the heat demand of the digester.
195 To give an upgraded layout, the MGT case which considers a novel integration of SOFC and
196 micro gas turbine in the SMAT plant is proposed. In the latter case, the boiler is replaced with
197 a micro gas turbine to provide a part of digester thermal energy demand.

198 ## 3.1 Base Case

199 The exhaust gas exiting from three SOFC units (streams 14a, 14b and 14c) are used in three
200 exhaust heat recovery exchangers (HXa, HXb and HXc) to heat up a hot water loop (stream 1).
201 Then an intermediate closed loop (first loop) is embedded to deliver the recovered heat to a
202 fraction of the sludge feeding the anaerobic digester (stream 7) flowing to the anaerobic
203 digester using a heat exchanger (HX1). When the recovered heat from the SOFC plant is not
204 sufficient to heat up the total amount of sludge and meet whole digester thermal load, an
205 auxiliary boiler is also used. Thus, to provide the digester with the required heat for the
206 digestion process, an amount of natural gas/biogas (streams 9a and 9b) is burned in an auxiliary
207 burner with excess air (stream 10). The second water loop distributes by means of a heat
208 exchanger (HX2) the heat from the boiler to the remainder of the sludge flow (stream 6) using.
209 Finally, a mixer is used to mix two sludge streams in a single stream, which is then fed into the

anaerobic digester [18]. Detailed schematic description of the base and MGT cases are presented in the following subsections.

3.2 MGT Case

The main difference between the MGT Case (Figure 4b) and the Base Case (Figure 4a) is that in the MGT Case the boiler is replaced with a microturbine operated in CHP mode to supply the heat that is is required for preheating the sludge. An heat exchanger (HX4) is employed to transfer thermal energy from the third loop to the sludge. Then the partially heated sludge is heated up to the required temperature by means of the boiler and second loop. The excessive amount of as-produced biogas which is not fed into SOFC systems are sent to microturbine. When the available biogas is not enough for both SOFC and the microturbine systems, an external amount of natural gas (NG) is supplied from the grid.

Figure 4a. Schematic of the DEMOSOFC plant.

Figure 4b. Proposed flowsheet for the biogas fed SOFC plant integrated with microturbine.

4. System analysis

Thermodynamic and techno-economic modeling of the above cogeneration systems (Base Case and MGT Case) are presented in this section.

4.1. Energy analysis

4.1.1 Assumptions

The following assumptions were used for simulation of the previosuly described plant condfigurations [18,19]:

- The atmospheric air is composed of 79% N_2 and 21% O_2, on a volume basis.
- All gases are treated as ideal gases and gas leakage is negligible.

• Internal distribution of temperature, pressure, and gas compositions in each component is uniform.

• Cathode and anode temperatures are assumed to be identical.

• The exhaust mass flow rates and temperatures of the three SOFC units are identical.

• Changes in the kinetic and potential energies of fluid streams are negligible.

• The biogas supplied to the SOFC contains 65% CH_4 and 35% CO_2 according to the reported data by SMAT Collegno [15].

• For each of the compressors, pumps, blowers, and turbines, proper isentropic efficiencies are considered.

4.1.2 Solid oxide fuel cell modeling

DC power is produced in SOFC via electrochemical processes. The methane gas existing in the biogas is reformed inside the anode side, producing mostly hydrogen which is oxidized in the SOFC. The following reforming, shift and overall electrochemical reactions take place at the cell anode electrode.

$$CH_4 + H_2O \rightarrow CO + 3H_2 \quad \text{(Reforming)} \tag{1}$$

$$CO + H_2O \rightarrow CO_2 + H_2 \quad \text{(Shifting)} \tag{2}$$

$$H_2 + \frac{1}{2}O_2 \rightarrow H_2O \quad \text{(overall electrochemical reaction)} \tag{3}$$

The molar conversion rates for reforming, shifting and electrochemical reactions are considered to be x_r, y_r, and z_r, respectively. Therefore, rates of consumption and production of the components can be achieved by the following model:

$$x_r \rightarrow \left[CH_4 + H_2O \rightarrow CO + 3H_2\right] \quad \text{(Reforming)} \tag{4}$$

$$y_r \rightarrow \left[CO + H_2O \leftrightarrow CO_2 + H_2\right] \quad \text{(shifting)} \tag{5}$$

$$z_r \rightarrow \left[H_2 + \frac{1}{2} O_2 \rightarrow H_2O \right] \quad \text{(Overall electrochemical reaction)} \tag{6}$$

250 z_r could be found with the help of current density, Faraday constant, cell number, and active
251 surface area, as followed by equation (7)

$$z_r = \frac{j \cdot N_{FC} \cdot A_a}{2 \cdot F} \tag{7}$$

252 Applying mass balance equations along with considering equations for the mixing units and
253 the whole SOFC model, the flowing gas compositions may be achieved. In order to solve the
254 system of equations, 3 more equations are needed to complete the system.
255 Looking again in the equilibrium reactions of shifting and reforming, the equilibrium constants
256 can be written as follows respectively:

$$\ln K_s = -\frac{\Delta \bar{g}_s^o}{\bar{R} T_{FC,e}} = \ln \left[\frac{(\dot{n}_{CO_2,8} + y_r) \times \left(\dot{n}_{H_2,8} + 3x_r + y_r - z_r \right)}{\left(\dot{n}_{CO,8} + x_r - y_r \right) \times \left(\dot{n}_{H_2O,8} - x_r - y_r + z_r \right)} \right] \tag{8}$$

$$\ln K_R = -\frac{\Delta \bar{g}_R^o}{\bar{R} T_{FC,e}} = \ln \left[\frac{(\dot{n}_{CO,8} + x_r - y_r) \times \left(\dot{n}_{H_2,8} + 3x_r + y_r - z_r \right)^3}{\left(\dot{n}_{CH_4,8} + x_r \right) \times \left(\dot{n}_{H_2O,8} - x_r - y_r + z_r \right) \times \dot{n}_9^2 \left(\frac{P_9}{P_{ref}} \right)^2} \right] \tag{9}$$

257 Where, $\bar{R}$ and $T_{FC,e}$ are the universal gas constant (8.314 J.mole^{-1}.K^{-1}) and the temperature at the
258 exit of the SOFC, respectively. Also, $\Delta \bar{g}^o$ is the change in the Gibbs free function of shifting
259 and reforming reactions.

$$\dot{W}_{FC,stack} = \sum_k \dot{n}_{k,9} \bar{h}_{k,9} + \sum_L \dot{n}_{L,4} \bar{h}_{L,4} - \sum_m \dot{n}_{m,8} \bar{h}_{m,8} - \sum_n \dot{n}_{n,3} \bar{h}_{n,3} \tag{10}$$

260 Where, k, L, m and n are the corresponding gas compositions in each states (e.g. gas
261 composition at state 9 (k) is CO_2, CO, H_2O, CH_4, N_2 and H_2)). On the other hand, the work rate
262 produced by the SOFC stack $\dot{W}_{FC,stack}$ can be expressed as:

$$\dot{W}_{FC,stack} = N_{FC} \cdot j \cdot A_a \cdot V_c \tag{11}$$

Where cell voltage is defined as:

$$V_c = V_N - V_{loss} \tag{12}$$

Here, V_N is the Nernst voltage and V_{loss} the voltage loss, which is the sum of three separate voltage losses; Ohmic, Activation and Concentration losses:

$$V_{loss} = V_{ohm} + V_{act} + V_{conc} \tag{13}$$

The Nernst voltage which is accounted as the ideal voltage can be expressed as;

$$V_N = -\frac{\Delta \bar{g}^o}{2F} + \frac{\bar{R}T_{FC,e}}{2F} \ln\left(\frac{a_{H_2}^{Anode,exit} \sqrt{a_{O_2}^{Cathode,exit}}}{a_{H_2O}^{Anode,exit}} \right) \tag{14}$$

In equation (14), the Gibbs energy difference is related to the overall electrochemical reaction. To determine the actual cell voltage, the voltage losses should be calculated. To calculate the Ohmic loss the following formula is used (See also

Table 1):

$$V_{ohm} = (R_{Int} + \rho_{an} L_{an} + \rho_{cat} L_{cat} + \rho_{ely} L_{ely})\, j \tag{15}$$

Table 1. Material Resistivity used for Ohmic voltage loss estimation [21]

The activation polarization is the sum of those defined for both the anode and cathode as follows;

$$V_{act} = V_{act,a} + V_{act,c} \tag{16}$$

$$V_{act,a} = \frac{\bar{R}T_{FC,e}}{F} (\sinh^{-1}(\frac{j}{2j_{oa}})) \tag{17}$$

$$V_{act,c} = \frac{\bar{R}T_{FC,e}}{F} (\sinh^{-1}(\frac{j}{2j_{oc}})) \tag{18}$$

Where j_o is the exchange current density. Eqs. (19) and (20) are used to evaluate the values of the exchange current density for the anode and the cathode, (see variables in Table 2), respectively [21].

$$j_{0,a} = \gamma_{an} \left(\frac{RT}{2F}\right) e^{\left(-\frac{E_{a,an}}{\bar{R}T}\right)} \tag{19}$$

$$j_{0,c} = \gamma_{cat} \left(\frac{RT}{2F}\right) e^{\left(-\frac{E_{a,cat}}{\bar{R}T}\right)} \tag{20}$$

Table 2. Parameters correspond to the material anode and cathode sides [21]

Concentration loss is sum of the losses related to gas concentration occurring in the anode and the cathode.

$$V_{conc} = V_{conc,a} + V_{conc,c} \tag{21}$$

where

$$V_{conc,an} = \frac{RT}{2F} \ln\left(\frac{P_{H_2} \times P_{H_2O,TPB}}{P_{H_2O} \times P_{H_2,TPB}}\right) \tag{22}$$

And

$$V_{conc,cat} = \frac{RT}{4F} \log\left(\frac{P_{O_2}}{P_{O_2,TPB}}\right) \tag{23}$$

where the subscript *TPB* denotes the three-phase boundary.

4.1.3 Energy demand of the reference plant

Explanation and values used for calculating the thermal terms are given in Table 3 and Figure 5a. Figure 5b shows the calculated total electrical demand of the wastewater treatment demand (SMAT Collegno) and thermal energy demand of the digester for 2015. As the figure indicates, during the summer months the required thermal and electrical demands are lower than those for the other months. The energy requirements for wastewater treatments plant are

characterized by a fluctuating demand for electricity from the process plant equipment, illumination, etc. These significant variations are mainly due to a fluctuations on the wastewater inflow during the year. Heating is mainly required for boosting the anaerobic reaction in anaerobic digester. In this work, space heating for the buildings in the plant is not considered as energy demand. The average amount of electrical power and thermal load demands are 723.13 kW and 281.12 kW respectively.

The digester thermal load (Q_{dig}), expressed in kW, is calculated as the sum of the following contributions:

- the thermal power required for the heating up sludge from a variable inlet temperature (14 - 23°C) to the digester temperature (38 - 47°C), Q_{sl}
- the extra heating of sludge that is required to compensate for heat losses through the digester walls, Q_{los}
- the heat losses though piping, Q_{pipes}

$$Q_{dig} = Q_{sl} + Q_{los} + Q_{pipes} \quad (24)$$

The first term in (Eq.25) is calculated based on:

- the sludge flow rate $\dot{m}_{sl}$ (the average monthly value is used as calculated from the SMAT hourly measurements)
- the sludge inlet temperature $T_{sl,in}$ (taken from the WWTP measurements)
- the digester process temperature T_{dig} (the average monthly value is taken, which is calculated from the SMAT daily measurements)
- being the solid content in sludge lower than 2% (weight), the specific heat capacity is calculated, c_p, is taken as equal to that of water.

The sludge pre-heating term is written as:

$$Q_{sl} = \dot{m}_{sl} \cdot c_p \cdot \left(T_{dig} - T_{sl,in}\right) \quad (25)$$

313 The digester thermal losses have been evaluated using (Eq. 27):

$$Q_{los} = Q_{ug} + Q_{ext} \quad (26)$$

314 Where:

$$Q_{los} = Q_{ug} + Q_{ext} \quad (27)$$

$$Q_{ug} = U_{ug} \cdot A_{ug} \cdot \left(T_{dig} - T_{gr}\right) \quad (28)$$

$$Q_{ext} = U_{ext} \cdot A_{ext} \cdot \left(T_{dig} - T_{ext}\right) \quad (29)$$

315 $Q_{ug}$is the term for losses through the underground surface (heat exchange between walls and
316 ground). Q_{ext} accounts instead for losses though the external surface (heat exchange between
317 walls and external air).
318 Finally, the thermal through piping has been evaluated as a fixed share of the total sludge pre-
319 heating duty and digester thermal losses:

$$Q_{pipes} = \%_{pipes} \cdot (Q_{sl} + Q_{los}) \quad (30)$$

320 The values used for the thermal load calculation are listed in Table 3.

321 Table 3. Main parameters for digester thermal load calculations.

322

323 Figure 5a. Sludge inlet, air and ground temperature trend.

324 The digester thermal load will be covered partially by the SOFC heat recovery system and
325 partially by the boiler. The boiler will be fed first with extra-biogas and then with NG from the
326 grid.

327 Figure 5b. Trends of total electrical demand and required thermal energy for digester in SMAT Collegno
328 calculated for 2015.

329 In the current operational condition of the plant, no cogeneration is in service. Therefore biogas
330 is used to supply heat to the digesters and natural gas is burnt in a boiler if required. The heating
331 demand is calculated by a steady state energy balance in both digesters.

332 ***4.1.4 Energy efficiency***

333 The energy efficiency for the overall system has been defined as follows:

$$\eta_I = \frac{\dot{W}_{net} + \dot{Q}_{recovery}}{\dot{m}_{biogas} \cdot LHV_{biogas} + \dot{m}_{NG} \cdot LHV_{NG}} \quad (31)$$

334 Where $\dot{W}_{net}$ is the net electrical power (stack AC power plus net MGT electrical power minus
335 the blowers and pumps power consumptions) and $\dot{Q}_{recovery}$ is the total heat recovered of the
336 system. In the denominator, there is the sum of the biogas consumption and the NG
337 consumption in the whole system.

338 ***4.1.5 SOFC model validation***

339 In order to validate the simulation results of SOFC, the available experimental data reported
340 by Tao et al. [22] is used. Table 4 compares the cell voltage and power density obtained in the
341 present model developed by the authors and those reported by Tao et al. [22]. The comparison
342 shows a good agreement between them.

Table 4. Comparison of results obtained from the present work with the experimental values reported by Tao et al. [22]

343

344 **4.2 Economic analysis**

345 Starting from the energy analysis on the four proposed scenarios, the economic analysis has
346 been performed to idetnify the best layouts from the economic perspective. The analysis is
347 based on the calculation of investment and operational costs. We calculate the cash flow trend
348 over the system lifetime. Pay Back Time (PBT) and Levelized Cost of Electricity (LCOE) are
349 used as economic indicators for the analyzed scenarios.

350 Capital costs have been calculated for the main plant sections.

- Biogas processing unit: this section is used to remove contaminants from the raw biogas. The clean-up unit is based on adsorption on activated carbon beds, as designed for the DEMOSOFC project. The cost has been taken from a recent workshop on cleaning systems for stationary fuel cell applications, promoted by the Argonne National Laboratory (US), where the most relevant fuel cell and cleaning system producers discussed on performance and price of the biogas processing system [23]. Costs are available for three-time scenarios and are expressed as a function of the fuel cell electrical power: today (1,500 €/kWe), short term (1,000 €/kWe) and long term (500 €/kWe).
- SOFC modules: Each module includes both the stacks and BoP. Each module produces AC power and hot water from purified biogas and ambient air. The choice of using a unique cost for all the module is due to the current commercial availability of SOFC modules for producers. The costs have been taken from a 2015 report developed by the European Fuel Cell and Hydrogen Joint Undertaking (FCH-JU) on the status of stationary fuel cell systems [24]. Data are available based on manufactured units and are shown in Figure 6. Because of the slightly different SOFC module size of the present work (60 kWe each), the specific cost (€/kWe) has been derived from the report and used for the analysis. Three scenarios have been defined to account for technology learning of the SOFC: today, short term and long term (Figure 6).
- Heat recovery system: Most of the components shown in the heat recovery layout are already installed in the WWTP for the sludge heating line through the boiler (current scenario). Furthermore, the MGT heat recovery system has been considered as included in the MGT investment cost. The only new component, which has been considered in the analysis, is the sludge-water heat exchanger (named HX1 in Figure 4a and 4b), which should be installed to recover heat from the SOFC section. The cost for this

component (shell and tube) has been derived from a simulation on Aspen Heat Exchanger Design and Rating® software. The simulation is based on available data on the hot water stream (1 kg/s, cooled from 72 to 40 °C on nominal conditions) and the sludge stream (0.886 kg/s, heated from 16 to 52 °C on nominal conditions). Hot stream has been assumed to be on tube side. The final cost for the heat-exchanger is 10,760 €.

- Micro gas turbine: The cost for a complete MGT system, equipped with heat recovery system, has been tttaken from Capstone [25] and is 1,000 €/kWe by averaging the values available. No technology learning has been adopted since the technology is already mature.

Figure 6. Specific investment cost for a 50 kWe unit and share among the cost components (stack, added system and installation). Author own elaboration of [24].

The operating costs have been also calculated during the plant lifetime (which has been assumed equal to 15 years for all the scenarios):

- Biogas processing unit. The specific operational cost, due to the replacement of the sorbent materials, is given for the same three time scenarios as function of the electrical energy produced by the fuel cell system: today (1.00 c€/kWhe), short term (1.00 c€/kWhe) and long term (0.50 c€/kWhe), as derived from [23].
- SOFC module unit. The operating costs for the module are expressed as yearly general maintenance and stack substitution according to lifetime, for the three time scenarios [24]. Stack lifetime is considered improved in the future scenarios from 3/4 to 5 to 7/8 years. Table 5 shows SOFC-related costs.
- Micro-gas turbine. The cost has been assumed as an average value from [25], and is equal to 1 c€/kWh.

- Natural gas. The cost of energy is related to the natural gas employed in the system for the boiler, the SOFC and the MGT. the cost of the natural gas is the one declared from the SMAT Collegno WWTP, equal to 0.6 €/m^3 (standard cubic meter) [15].
- Savings. No specific subsidy for electricity production from biogas has been considered. From the Italian legislation on feed-in-tariff for energy production from renewables [26], in the case of biogas from sewage sludge, the tariff is lower than the current price of electricity in the WWTP. For this reason, if the energy is required internally, the most convenient choice is to have self-consumption. The savings are thus accounted using the electricity price in the SMAT Collegno WWTP, equal to 16 c€/kWhe [15]. Savings are accounted as constant during the entire lifetime except for the first year, where 6 months of construction have been considered with a related 50% reduction in the yearly savings.

Table 5 summarize the investment and operating costs for the biogas processing unit, the SOFC module and the MGT.

Table 5. SOFC, biogas processing unit and MGT costs. [23] [24] [25]

Starting from the investment and the operational costs, the yearly cash flow can be evaluated. The methodology is explained in detail in the authors' previous work [27]. The discount rate has been assumed 2.5% (assumptions, the value used for discounting future costs and savings) and tax rate 24% (from the Italian previsions on industry for 2017. Taxes are applied to the net yearly cash flow, in case it is positive). The analysis has been done for a 15 years' period for all the analyzed scenarios.

The economic indicators are the standard Pay-back time (PBT: the first year in which the cumulated yearly cash flow is positive) and the Levelized cost of electricity (LCOE), defined

as the ratio between the total discounted lifetime costs (investment and operational) and the total discounted electrical energy production:

$$LCOE = \frac{\sum_{i=1}^{N} \frac{C_{inv,i} + C_{op,i}}{(1+r)^i}}{\sum_{i=1}^{N} \frac{E_i}{(1+r)^i}} \quad (32)$$

where:

$C_{inv,i}$ are the yearly investment costs

$C_{op,i}$ are the yearly operational costs

E_i is the net yearly energy production

r is the discount rate

N is the system lifetime

The matrix of the analyzed case studies is shown in Table 6.

Table 6. Matrix of the analyzed case studies.

5. Results and discussion

To compare the performance of MGT case with that of the base case, required natural gas, covered thermal load of the digester, produced electrical power, system efficiency, as well as the results of economic analysis for both cases, are presented in this section. In addition, for the MGT case, four different scenarios using Capstone microturbine systems are developed to show which arrangement of the commercial products can be appropriate to cover the thermal demand of digester. To take the final decision, economic analysis results as well as those of the energy analysis will reveal the best choice among the scenarios.

5.1. Energy simulation results

For each SOFC module, 60 kW of electrical power is produced, so the amount of biogas required for feeding the SOFC modules is constant throughout the year.

NG and biogas consumptions (Figure 7a) in the boiler of the plant are calculated for the base case using the calculated data of digester thermal energy demand. The results are illustrated in Figure 7a, showing that the required NG in the boiler is lower than the available biogas (the portion of the produced biogas which is not fed into the SOFC system). As shown in the figure, during summer the available biogas is very low and thus NG consumption from the grid increases. The annual NG and biogas consumptions in the boiler are calculated to be 33,717 Nm^3 and 165,411Nm^3, respectively.

As shown in Figure 7b, the required amount of NG in the boiler increases when the system is equipped with MGT (instead of the simple boiler in the base case system). The increase in NG consumption is because by exploitation of the microturbine system in place of the boiler, the plant is supposed to produce electricity power along with meeting the thermal energy demand of digester simultaneously, so it is expected to burn more fuel in the combustion chamber of MGT system. The annual NG consumption for the MGT case is increased by up to 300% compared to the Base case.

Figure 7. Natural gas and biogas consumptions in the boiler for a) the Base Case b) the MGT Case

In the Base Case configuration, the SOFC systems are the sole producers of the electrical power. However, in the MGT case, additional electrical power is produced using the microturbine as shown in Figure 8. Referring to the results shown in Figure 8, the produced electrical power by microturbine shows a decreasing trend from January to August and increasing trend for the next following months. Since the microturbine is governed in order to supply the heat demand of the digester and considering that the heat demand is low during summer season, the produced power follows the same trend of the heat demand.

Figure 8. Electrical power demand and production in the proposed MGT integrated plant (MGT Case).

Figure 9 shows the total efficiency for both the base and the MGT cases. Referring to the figure, it is found that although the NG consumption of the MGT case system is higher than that of the base case system (Figure 7), the total efficiency for the MGT case is always higher due to the extra electrical power production for this case. In addition, it should be noted that, when the heat demand for the digester is higher, the difference in efficiency between the two cases becomes more.

Figure 9. System efficiency for the Base Case and MGT Case.

It can be concluded that from the energy analysis results, using the MGT system instead of the boiler would be effective as the system efficiency and also coverage of electrical demand of the plant (SMAT Collegno) increase. In the following, using commercial MGT systems from Capstone Company [13], four scenarios are proposed (Table 7). Two MGT systems, namely C30 and C65 which are rated to produce net electrical power of 30 kW and 65 kW are chosen [28]. The reason for choosing these two units is their thermal heat recovery potentials by which the system could meet the required thermal demand of digester.

Operation under a partial load (PL) condition was also considered in this study. Outputs of MGT-30 and MGT-65 at partial load condition can be obtained using the following equations reported in Ref. [13]. Electrical power output P_e, recovered exhaust heat Q_{ehr}, and fuel flowrate Q_{fuel} for MGT-30 and MGT-65 models under partial load conditions (PL) can be estimated by Eqs. (33-38) as function of the full load (FL) conditions.

$$\dot{W}_{MGT-30,PL} = \dot{W}_{MGT-30,FL} \times PL \tag{33}$$

$$\dot{Q}_{ehr,MGT-30,PL} = \dot{Q}_{ehr,MGT-30,FL}(0.1718 + 0.6529 \times PL + 0.1706 \times PL^2) \tag{34}$$

$$\dot{Q}_{fuel,MGT-30,PL} = \dot{Q}_{fuel,MGT-30,FL}(0.1513 + 0.7824 \times PL + 0.06004 \times PL^2) \tag{35}$$

$$\dot{W}_{MGT-65,PL} = \dot{W}_{MGT-65,FL} \times PL \tag{36}$$

$$\dot{Q}_{ehr,MGT-65,PL} = \dot{Q}_{ehr,MGT-65,FL}(0.1240 + 0.9707 \times PL - 0.1706 \times PL^2) \quad (37)$$

$$\dot{Q}_{fuel,MGT-65,PL} = \dot{Q}_{fuel,MGT-65,FL}(0.1228 + 0.9766 \times PL - 0.1131 \times PL^2) \quad (38)$$

In the first two scenarios (Scenario A and B) all the units are considered to be worked at full load which means there is not any fluctuation in power production so that in scenario A and B, the systems can produce 275kW and 310kW electrical power respectively. For the last two scenarios (Scenario C and D) the MGT should be governed in such a way that the heat demand of digester is supplied by means of exhaust thermal potential of MGT and consequently during some months MGTs are supposed to work at partial load rather than full load. As mentioned before, the SOFC units are operating under full load condition. Table 7 presents the configuration of the different scenarios.

Table 7. Configurations and operating conditions of the investigated scenarios.

5.1.1 Scenario A

In full load conditions C65 and C30 can produce 105 kW and 56 kW thermal energy respectively [13]. For Scenario A, the SOFC system, C65 and C30 are working at full load so as can be seen in Figure 10a thermal load produced by MGT from March to December is quite more than the required heat demand. However, as shown in Figure 10b, the produced electrical power would be less than that of the MGT Case from January to May and more than it from Jun to October. Meanwhile, results reveal that annual average electrical power production for Scenario A would be 5.54% more compared to the MGT Case. The results show that using this Scenario, the plant can cover almost 38% of total electrical power demand of SMAT Collegno. However, looking at the total efficiency results shown in Figure 10c, it can be observed that total efficiency is lower even compared to the base case due to higher consumption of NG and consequently more waste heat is produced from May to November. The average system

efficiency for this scenario is 6.36% and 14.4% lower than that for the Base Case and MGT Case respectively.

Figure 10. a) Thermal load, b) Electrical power and c) Total efficiency for Scenario A.

5.1.2 Scenario B

The results calculated for Scenario B are illustrated in Figure 11. Referring to Figure 11a, for almost all along the year produced heat is exceeding the required heat for the digester. Consequently, the NG consumption should be higher than that for the Scenario A and also the electrical net power would be more than that of the scenario A. However, the results of total efficiency still unfold that the system efficiency for Scenario B is lower than that for Base Case and MGT Case by 7.4% and 15.4% respectively. This shows that despite having higher electrical power production. The negative effect of NG consumption overcomes the positive effect of produced electrical power. Nevertheless, using this scenario reveals that 42.8 % of total required electrical demand of the SMAT can be produced.

Figure 11. a) Thermal load, b) Electrical power and c) Total system efficiency for Scenario B

5.1.3 Scenario C

As discussed earlier, for Scenario C and D the MGT is governed in order to provide the needed heat demand of digester. For scenario C in which C30 unit and C65 unit are supposed to be implemented, for some months (from Jan to May and from October to December) C65 unit works at full load; however, for the rest the systems should work in partial load (Figure 12). On the other hand, C30 unit should be turned off from Jun to November as during these months C65 unit could produce enough thermal load to supply the required heat in the digester. The decision on when to have C65 at full load, when C30 is off, has been taken to better fit the thermal load. The produced electrical power and system efficiency curves found for this

scenario are close to those of the case MGT Case particularly from May to November. In January, the difference between the MGT Case and this scenario is because using both the C30 and C65 even at full load could not meet the needed heat demand of digester. The annual average efficiency for scenario C. is found 62.74%. Also, using this Scenario the possibility to cover the electrical demand of the plant will be 35.01%.

Figure 12. a) Thermal load, b) Electrical power and c) Total system efficiency for Scenario C

5.1.4 Scenario D

For the scenario D, the results are shown in Figure 13. Referring to Figure 13a, the thermal energy seems to be covered better than the other cases. By using two C65 it is found that almost 98% of required heat demand could be produced. Figure 13b shows the obtained results for electrical power which indicates that the electrical power could be produced more than in scenario C so the trend is closer to the MGT Case rather than scenario C. The electrical efficiency values (Figure 13c) are almost similar to the scenario C (Figure 12c). The annual average efficiency for scenario D is 65.15%, which is higher than the value of Scenario C. In addition, 36.17% of total required electrical demand can be covered in the plant.

Figure 13. a) Thermal load, b) Electrical power and c) Total system efficiency for Scenario D

5.2. Economic analysis results

The first part of the techno-economic analysis has been devoted to the analysis of the energy inputs to the system, on a yearly basis. As can be seen in Table 8, the SOFC size is kept constant at 180 kWe, while the MGT size is varying depending on the scenarios, from 0 to 210 kWe. According to the system size and the regulation strategy, the yearly NG consumption can be evaluated as the sum of the MGT consumption, SOFC consumption (only required to keep stable the SOFC operating point in case of reduced biogas production, e.g. during summer

559 months) and boiler use (in case of not complete coverage of the digester thermal load through
560 the system heat recovery). The highest natural gas consumption is related to the scenario B,
561 where the turbines have the highest size and are working at full load. The same turbine size,
562 with the partial load operation, has a reduction in natural gas consumption of 52.1%. A similar
563 reduction (46.5 %) can be noticed among scenarios A and C, where the partial load is applied
564 to the smallest turbine size.

565 Table 8. Electrical and natural gas yearly consumption for the different scenarios.

566 The power production from the system has been compared to the WWTP electrical and thermal
567 loads. The electrical coverage, thanks to the MGT installation, increases from 24.9% to a
568 maximum value of 42.9% in Scenario B (large ideal MGT at full load).
569 The digester thermal load coverage is also increased when the MGT integration is considered.
570 As can be seen in Table 8, the NG consumption for boiler feeding is reduced by 100% in case
571 of the ideal MGT Case, of 42% in scenarios A and C (C30+C65) and 84.6% in scenarios B and
572 D (C65+C65). Thermal recovery from MGT thus helps, besides in increasing the electrical
573 coverage, also in reducing the consumption of NG for thermal requirements.
574 From the analysis of the energy production in the different scenarios, the economic analysis
575 has been performed with the calculation of the PBT and LCOE.
576 Figure 14 shows the LCOE for the different scenarios and cost trajectories during the time.
577 Values should be compared with the current price of electricity in the WWTP, which
578 corresponds to 0.16 €/kWh [15]. As can be seen, the 'current' scenario leads to high LCOEs,
579 between 0.223 and 0.309 €/kWh for all the configurations: the cost of producing the electrical
580 kWh, in none of the proposed case studies, can be considered cheaper than buying electricity
581 from the grid, in a 15 years' period. The MGT introduction always leads to a positive effect on
582 the economic performance of the system: this is due to the relatively low investment costs
583 (compared to the entire plant) compared to the increase in the electrical production of the

584 system. Among the different scenarios, the ideal MGT case is the one with the lowest LCOE,
585 followed by scenario B and D with the 2xC65 gas turbines, working at full and partial load.
586 The short-term scenario, related to a 500 units production (cumulative per company, see Figure
587 6) brings to a strong reduction in the SOFC investment cost, and thus a better economic profile.
588 All LCOEs are now lower than the current price of electricity in the SMAT site (0.16 c€/kWh),
589 with values ranging from 0.116 to 0.134 €kWh. Again, the lower costs is related to the ideal
590 MGT case, followed by scenarios C and D, related to the partial load operations of the turbines.
591 The analysis on the long term scenario confirms the trend discussed for the other case studies,
592 with LCOE values in the range 0.088-0.102 c€/kWh.
593 The introduction of a MGT, respect to the SOFC-only Base Case, brings to a 12% reduction in
594 LCOE (from scenario MGT/C to A). Furthermore, in all the proposed configurations use of
595 partial load brings to a reduction in the LCOE of around 6%.
596 The second economic indicator, the payback time, varies from one scenario to another
597 according to the same trends discussed for the LCOE. For this reason, the two indicators are
598 compared only for the short term scenario (Table 9). The short term scenario, with a SOFC
599 investment costs of 5'656 €/kWe, has been considered the most promising and achievable
600 target, without any specific subsidy schemes, for SOFC systems. For this scenario, the
601 breakdown of LCOE among CAPEX and OPEX costs is provided. Results are shown in Table
602 9.
603 Figure 14. Levelized cost of electricity for the different scenarios and cost trajectories.
604 The highest LCOE of the SOFC-only case study (called 'Base case') is due to the high
605 investment cost of the technology about the electrical energy produced. The introduction of an
606 MGT leads to a higher increase in the energy produced respect to the increase in costs, and this
607 results in a lower LCOE. On the other side, operating costs are indeed similar for the SOFC
608 and ideal MGT cases, and slightly increasing for the real MGT scenarios (A, B, C, D) because

609 of the increase in the NG request. The payback time confirms this trends, with a value higher
610 than 11 years for the SOFC-only case, reduced at 7.66 in the ideal MGT one. When analyzing
611 real MGT scenarios, payback time are always between 7.9 and 8.5 years (reduction of 30%
612 respect to the SOFC-only base case). Use of partial operation for MGT is again confirmed as a
613 positive choice, which leads to a reduction in PBT of around 5%.
614 These values are strongly reduced in the long term economic analysis (SOFC cost equal to
615 2'326 €/kWe). Here, the low cost of the SOFC technology, reduces the positive effect of the
616 MGT, since they are able to provide similar electrical energy based on similar specific
617 investment costs, but with a lower efficiency. In this case, the payback time is ranging from
618 3.3 years (Scenario C) to 3.9 years (Base case).
619 From the complete economic analysis, it is pointed out that the MGT is able to increase the
620 economic benefits of the SOFC system, especially in the current and short term scenario where
621 the specific SOFC costs is still high (reduction in LCOE of 27.9 and 12.9% are found between
622 MGT and Base Case for Current and Short Term scenario). The advantages of installing a MGT
623 are reduced in the Long Term scenario (LCOE reduction of 1.3% between MGT and Base
624 Case). Furthermore, when a MGT is installed, the option of the partial load operation shows a
625 slightly better economic profile, while no essential differences are pointed out for the choice
626 of a C65+C30 or C65+C65 layout.
627 Table 9. LCOE and PBT for the different technical scenario, with a short term economic scenario.

628 # 6. Conclusion

629 Biogas produced in wastewater treatment plants is versatile renewable energy source that can
630 be efficiently transformed to heat or electricity and heat. Two plant configuraitons, namely
631 Base case and MGT case, are developed and analyzed for a wastewater treatment plant located
632 in Torino (IT). In both cases, the produced biogas from the digester of the plant is first sent to
633 the SOFC having an electrical capacity of 180 kW. In the Base case, thermal power recovered

from the exhaust of the SOFC systems along with an biogas/NG external boiler are used to cover the digester thermal load. casein the MGT case, the boiler is replaced with the micro gas turbine operated in CHP mode. For the MGT case, after getting the first-hand results, four scenarios using the commercial micro gas turbines of Capstone are proposed. The following conclusions could be drawn from this work;

- Results show that although using the micro gas turbines in the plant requires the increase in NG from the grid, the the overall efficiency of the plant is increased by up to 7% due to an increase in the total electrical power of the plant.
- Comparing the obtained results for the base case with those of MGT case reveals that overall electrical power of the MGT case is averagely 110 kW more than that of the base case system.
- Comparing the effect of using different arrangements of the commercial micro gas turbines for the MGT case shows that by using C30 and C65 in the governing mode a reduction of the coverage occurs, equal to 3% in case of small size (C30+C65 MGT) and 6.2% in case of the larger installation (C65+C65 MGT).
- The shortest investment recovery is obtained with the MGT case, followed by the other MGT scenarios (cased A to D), which show a PBT between 7.66 and 8.46 years in a the shortterm economic scenario. The addition of a MGT to the base case scenario always leads to a benefit in terms of economic indicators.
- The choice of working in partial load with the MGT shows better economic performance.

Finally, it can be declared that suggested proposal for using the micro gas turbine along with SOFC system in the wastewater treatment plant is beneficial.

References

[1] P.S. Forms, Horizon 2020 Call : H2020-JTI-FCH-2014-1 Type of action : FCH2-IA Proposal number : 671470 Proposal acronym : DEMOSOFC Table of contents, (2014).

[2] S.-H. Cui, J.-H. Li, A. Jayakumar, J.-L. Luo, K.T. Chuang, J.M. Hill, et al., Effects of H2S and H2O on carbon deposition over La0.4Sr0.5Ba0.1TiO3/YSZ perovskite anodes in methane fueled SOFCs, J. Power Sources. 250 (2014) 134–142. doi:10.1016/j.jpowsour.2013.10.124.

[3] G.J. Williams, A. Siddle, K. Pointon, Design optimisation of a hybrid solid oxide fuel cell and gas turbine power generation system, Harwell Laboratory, Energy Technology Support Unit, Fuel Cells Programme, 2001.

[4] D.F. Cheddie, R. Murray, Thermo-economic modeling of a solid oxide fuel cell/gas turbine power plant with semi-direct coupling and anode recycling, Int. J. Hydrogen Energy. 35 (2010) 11208–11215. doi:10.1016/j.ijhydene.2010.07.082.

[5] D.F. Cheddie, R. Murray, Thermo-economic modeling of an indirectly coupled solid oxide fuel cell/gas turbine hybrid power plant, J. Power Sources. 195 (2010) 8134–8140. doi:10.1016/j.jpowsour.2010.07.012.

[6] X. Zhang, Y. Wang, T. Liu, J. Chen, Theoretical basis and performance optimization analysis of a solid oxide fuel cell-gas turbine hybrid system with fuel reforming, Energy Convers. Manag. 86 (2014) 1102–1109. doi:10.1016/j.enconman.2014.06.068.

[7] Y. Bicer, I. Dincer, Energy and exergy analyses of an integrated underground coal gasification with SOFC fuel cell system for multigeneration including hydrogen production, Int. J. Hydrogen Energy. 40 (2015) 13323–13337. doi:10.1016/j.ijhydene.2015.08.023.

682 [8] Z. Yan, P. Zhao, J. Wang, Y. Dai, Thermodynamic analysis of an SOFC-GT-ORC
683 integrated power system with liquefied natural gas as heat sink, Int. J. Hydrogen
684 Energy. 38 (2013) 3352–3363. doi:10.1016/j.ijhydene.2012.12.101.

685 [9] Y. Inui, T. Matsumae, H. Koga, K. Nishiura, High performance SOFC/GT combined
686 power generation system with CO 2 recovery by oxygen combustion method, Energy
687 Convers. Manag. 46 (2005) 1837–1847.

688 [10] V. Eveloy, W. Karunkeyoon, P. Rodgers, A. Al Alili, Energy, exergy and economic
689 analysis of an integrated solid oxide fuel cell – gas turbine – organic Rankine power
690 generation system, Int. J. Hydrogen Energy. 41 (2016) 1–16.
691 doi:10.1016/j.ijhydene.2016.01.146.

692 [11] Y. Inui, S. Yanagisawa, T. Ishida, Proposal of high performance SOFC combined
693 power generation system with carbon dioxide recovery, Energy Convers. Manag. 44
694 (2003) 597–609. doi:10.1016/S0196-8904(02)00069-9.

695 [12] D. Sánchez, R. Chacartegui, T. Sánchez, J. Martínez, F. Rosa, A comparison between
696 conventional recuperative gas turbine and hybrid solid oxide fuel cell—gas turbine
697 systems with direct/indirect integration, Proc. Inst. Mech. Eng. Part A J. Power
698 Energy. 222 (2008) 149–159.

699 [13] M. Firdaus, B. Basrawi, T. Yamada, K. Nakanishi, H. Katsumata, Analysis of the
700 performances of biogas-fuelled micro gas turbine cogeneration systems (MGT-CGSs)
701 in middle- and small-scale sewage treatment plants : Comparison of performances and
702 optimization of MGTs with various electrical power outputs, Energy. 38 (2012) 291–
703 304. doi:10.1016/j.energy.2011.12.001.

704 [14] DEMOSOFC project official website, (n.d.).

705 [15] M. Gandiglio, A.S. Mehr, A. Lanzini, M. Santarelli, Design, Energy Modeling and

706 Performance of an Integrated Industrial Size Biogas Sofc System in a Wastewater
707 Treatment Plant, Proc. ASME 2016 14th Int. Conf. Fuel Cell Sci. Eng. Technol.
708 FUELCELL2016 June 26-30, 2016, Charlotte, North Carolina. (2016).

709 [16] Google Maps, (2016).

710 [17] P. Akbari, R. Nalim, Performance Enhancement of Microturbine Engines Topped, 128
711 (2006). doi:10.1115/1.1924484.

712 [18] A.S. Mehr, M. Gandiglio, M. MosayebNezhad, A. Lanzini, S.M. Mahmoudi, M. Yari,
713 et al., Solar-assisted integrated biogas solid oxide fuel cell (SOFC) installation in
714 wastewater treatment plant: energy and economic analysis, Appl. Energy. 191 (2017)
715 620–638. doi:10.1016/j.apenergy.2017.01.070.

716 [19] Z. Wuillemin, Experimental and modeling investigations on local performance and
717 local degradation in solid oxide fuel cells., Lab. Energy Syst. PhD (2009).
718 doi:10.5075/epfl-thesis-4525.

719 [20] A.S. Mehr, S.M.S. Mahmoudi, M. Yari, A. Chitsaz, Thermodynamic and
720 exergoeconomic analysis of biogas fed solid oxide fuel cell power plants emphasizing
721 on anode and cathode recycling: A comparative study, Energy Convers. Manag. 105
722 (2015) 596–606. http://linkinghub.elsevier.com/retrieve/pii/S019689041500744X.

723 [21] S. Wongchanapai, H. Iwai, M. Saito, H. Yoshida, Selection of suitable operating
724 conditions for planar anode-supported direct-internal-reforming solid-oxide fuel cell, J.
725 Power Sources. 204 (2012) 14–24. http://dx.doi.org/10.1016/j.jpowsour.2011.12.029.

726 [22] V.A. Tao G, Armstrong T, ntermediate temperature solid oxide fuel cell (IT-SOFC)
727 research and development activities at MSRI, in: ACERC&ICES Conf., Utah, 2005.

728 [23] Argonne National Laboratory, Gas Clean-Up for Fuel Cell Application Workshop,

729 (2014) 1–32.

730 [24] Roland Berger Strategy Consultants, Advancing Europe's energy systems: Stationary
731 fuel cells in distributed generation. A study for the Fuel Cells and Hydrogen Joint
732 Undertakinng, 2015. doi:10.2843/088142.

733 [25] J. Pierce, Capstone 30 kW and 60 kW microturbine installations at landfills, in:
734 Intermt. CHP Appl. Cent. Work. CHP Bioenergy Bioenergy Landfills Wastewater
735 Treat. Plants, 2005.

736 [26] Ministero dello Sviluppo Economico, Decreto 6 luglio 2012 - Attuazione dell'art. 24
737 del decreto legislativo 3 marzo 2011, n. 28, recante incentivazione della produzione di
738 energia elettrica da impianti a fonti rinnovabili diversi dai fotovoltaici, GU Ser. Gen.
739 N. 159 Del 10-7-2012 - Suppl. Ordin. N. 143. (2012) 1–65.

740 [27] F. Curletti, M. Gandiglio, A. Lanzini, M. Santarelli, Large size biogas-fed Solid Oxide
741 Fuel Cell power plants with carbon dioxide management : Technical and economic
742 optimization, 294 (2015).

743 [28] Capstone Products, (n.d.).

744 [29] F. Pizza, Welcome to Milano-Nosedo municipal WWTP The WWTP of Milano
745 Nosedo, (2015).

746 **Figures' caption**

747

748 Figure 1. SMAT wastewater treatment plant in Collegno (Turin) [16]. "DEMOSOFC Plant" shows the area
749 where the three SOFC modules will be installed.
750 Figure 2. Concept diagram of the DEMOSOFC plant [14].
751 Figure 3a. Proposed SOFC system layout.
752 Figure 4a. Schematic of the DEMOSOFC plant.
753 Figure 5a. Sludge inlet, air and ground temperature trend.
754 Figure 6. Specific investment cost for a 50 kWe unit and share among the cost components (stack, added system
755 and installation). Author own elaboration of [22].
756 Figure 7. Natural gas and biogas consumptions in the boiler for a) the Base Case b) the MGT Case
757 Figure 8. Electrical power demand and production in the proposed MGT integrated plant (MGT Case).

Figure 9. System efficiency for the Base Case and MGT Case.
Figure 10. a) Thermal load, b) Electrical power and c) Total efficiency for Scenario A.
Figure 11. a) Thermal load, b) Electrical power and c) Total system efficiency for Scenario B
Figure 12. a) Thermal load, b) Electrical power and c) Total system efficiency for Scenario C
Figure 13. a) Thermal load, b) Electrical power and c) Total system efficiency for Scenario D
Figure 14. Levelized cost of electricity for the different scenarios and cost trajectories.

Figures

Figure 15. SMAT wastewater treatment plant in Collegno (Turin) [16]. “DEMOSOFC Plant” shows the area where the three SOFC modules will be installed.

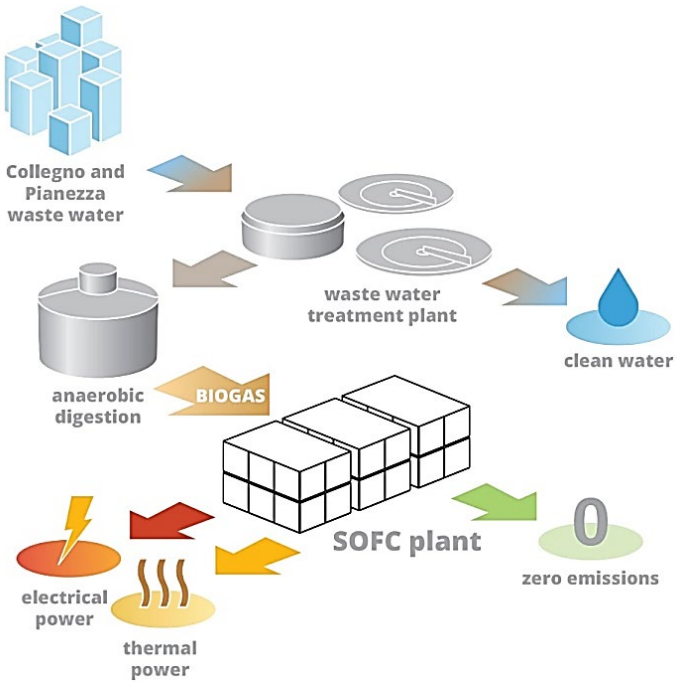

Figure 16. Concept diagram of the DEMOSOFC plant [14].

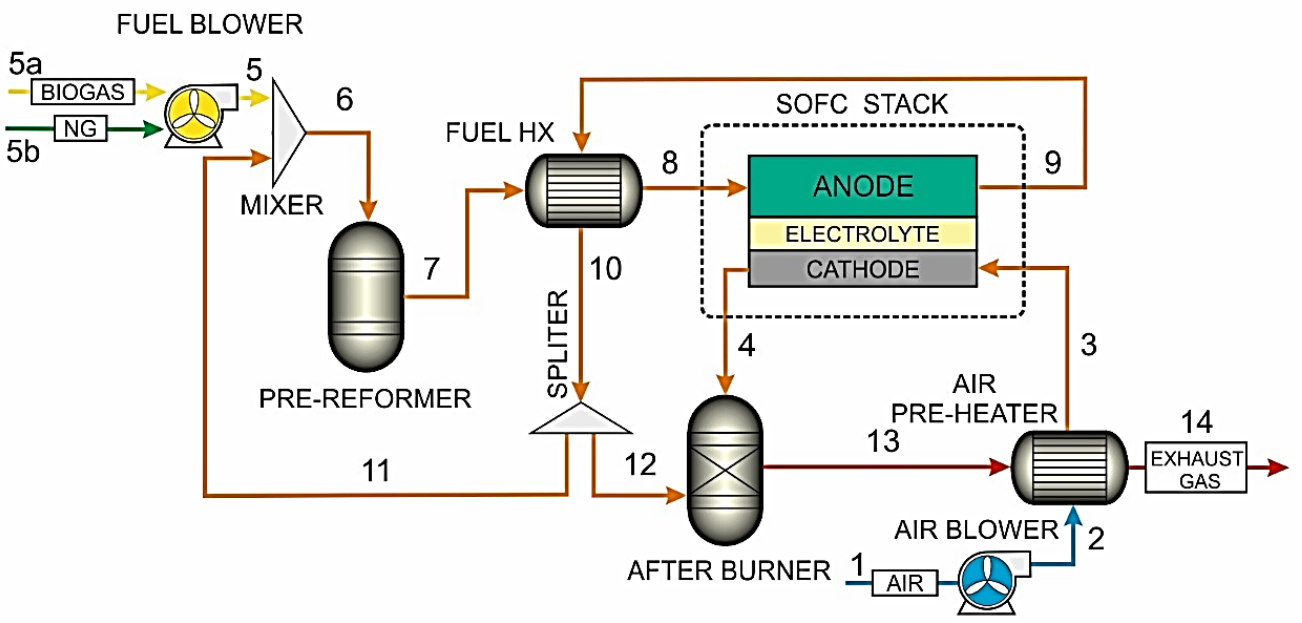

Figure 17a. Proposed SOFC system layout.

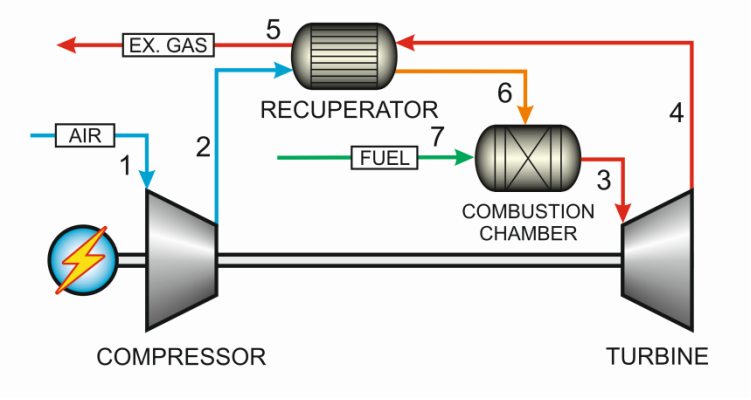

Figure 3b Schematic of the regenerated microturbine system

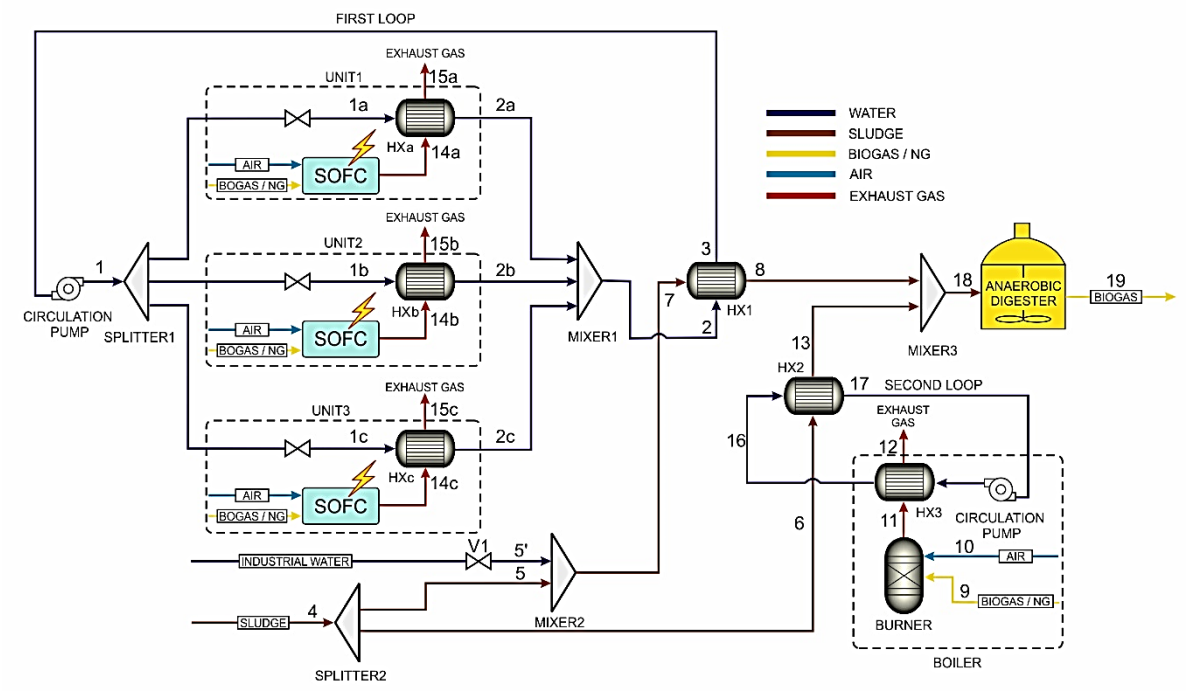

841

842 Figure 18a. Schematic of the DEMOSOFC plant.

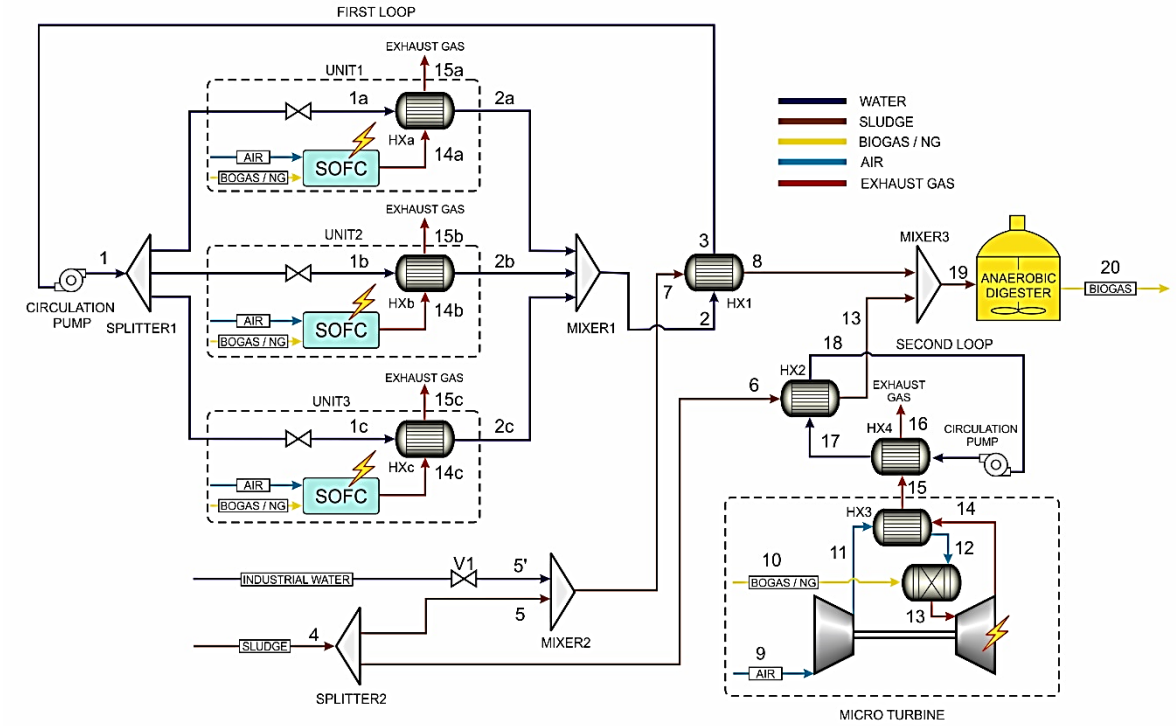

843

844 Figure 4b. Proposed flowsheet for the biogas fed SOFC plant integrated with microturbine.

845
846
847
848
849

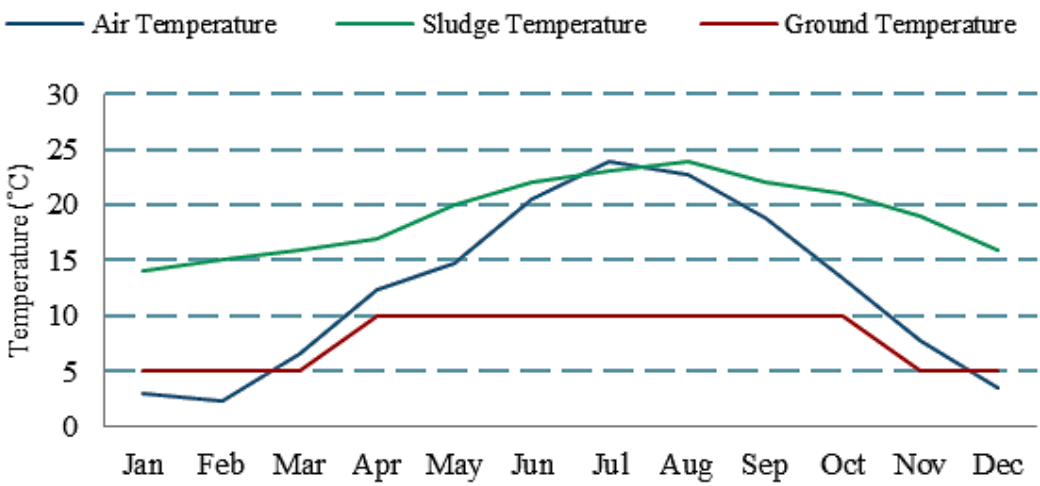

Figure 19a. Sludge inlet, air and ground temperature trend.

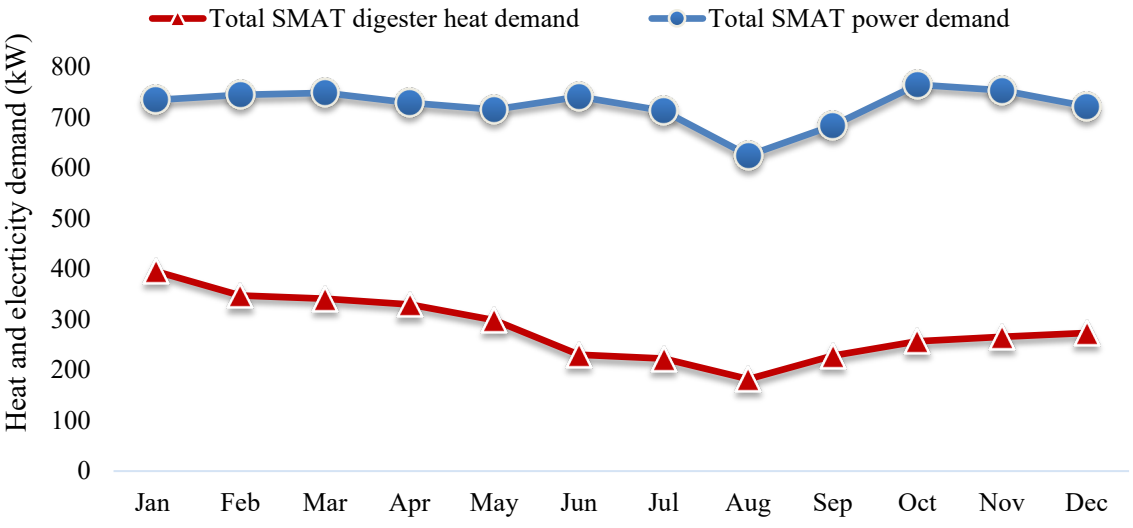

Figure 5b. Trends of total electrical demand and required thermal energy for digester in SMAT Collegno calculated for 2015.

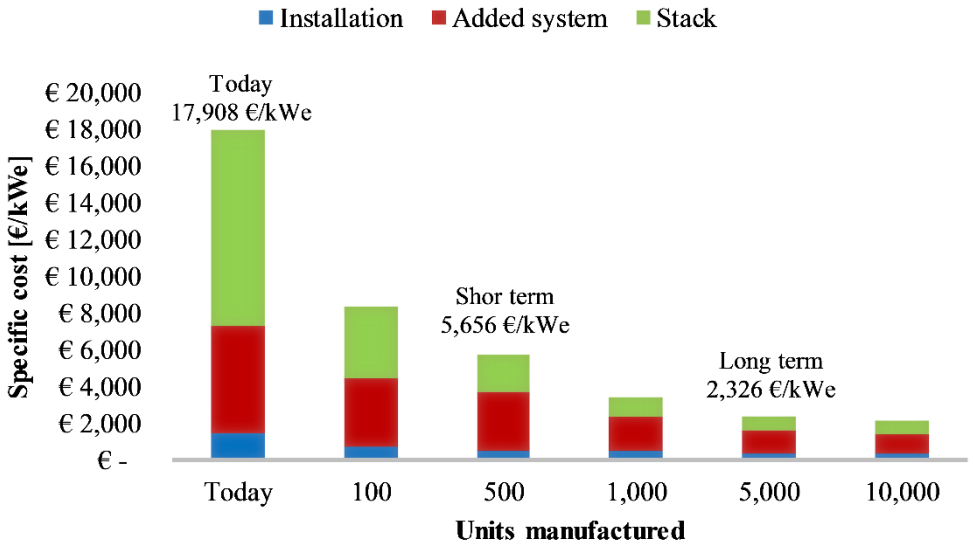

Figure 20. Specific investment cost for a 50 kWe unit and share among the cost components (stack, added system and installation). Author own elaboration of [24].

884

885

a)

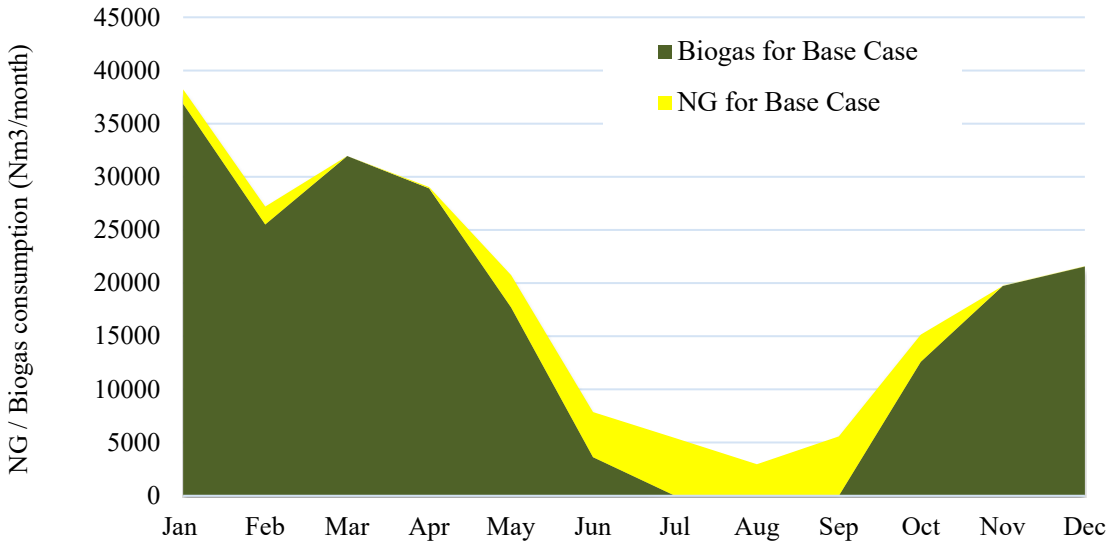

b)

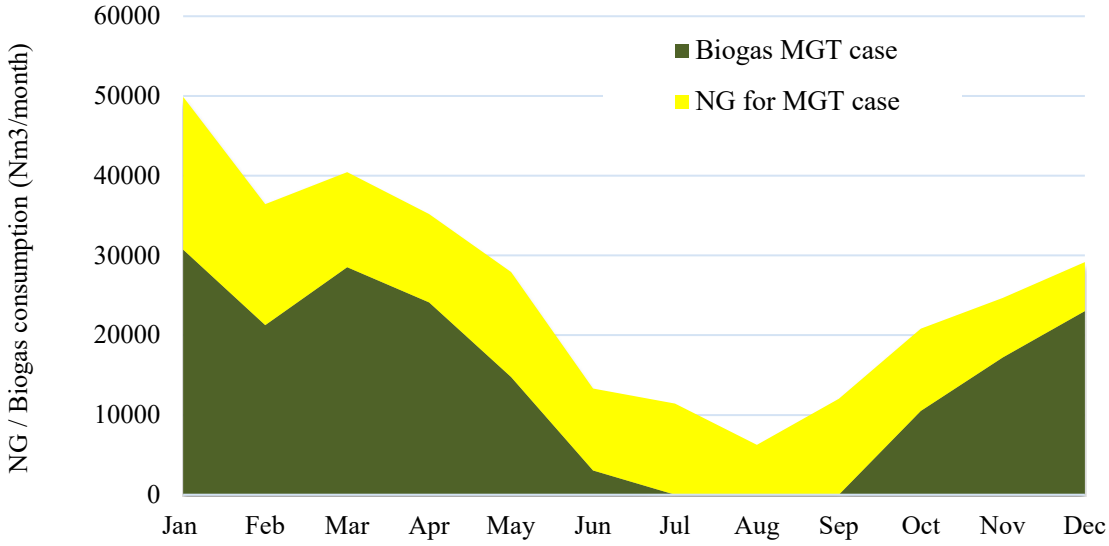

Figure 21. Natural gas and biogas consumptions in the boiler for a) the Base Case b) the MGT Case

886

887

888

889

890

891

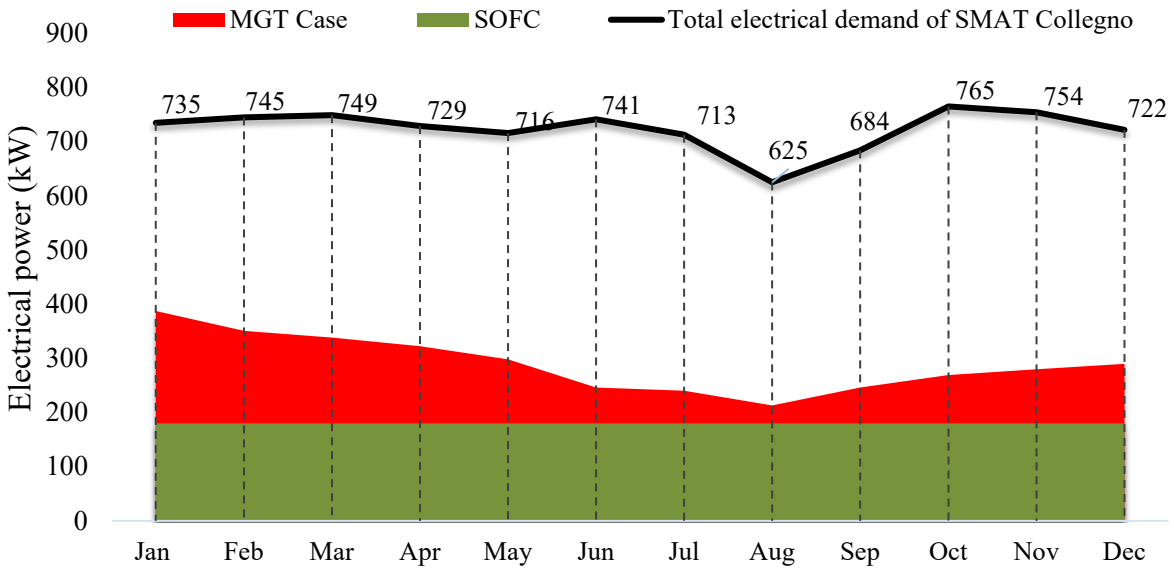

Figure 22. Electrical power demand and production in the proposed MGT integrated plant (MGT Case).

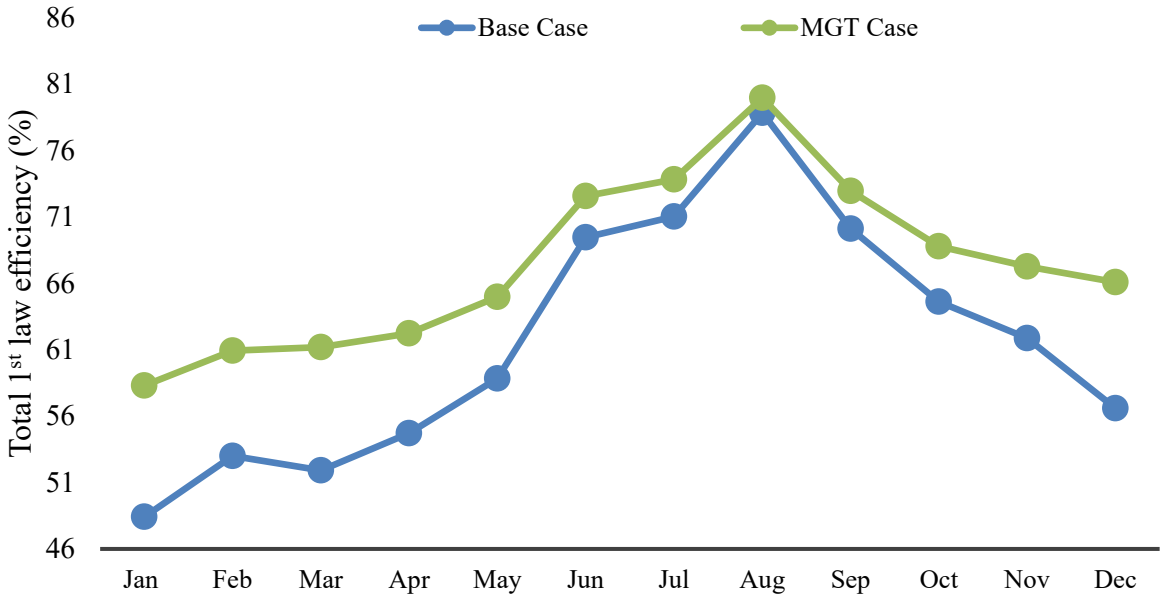

Figure 23. System efficiency for the Base Case and MGT Case.

a)

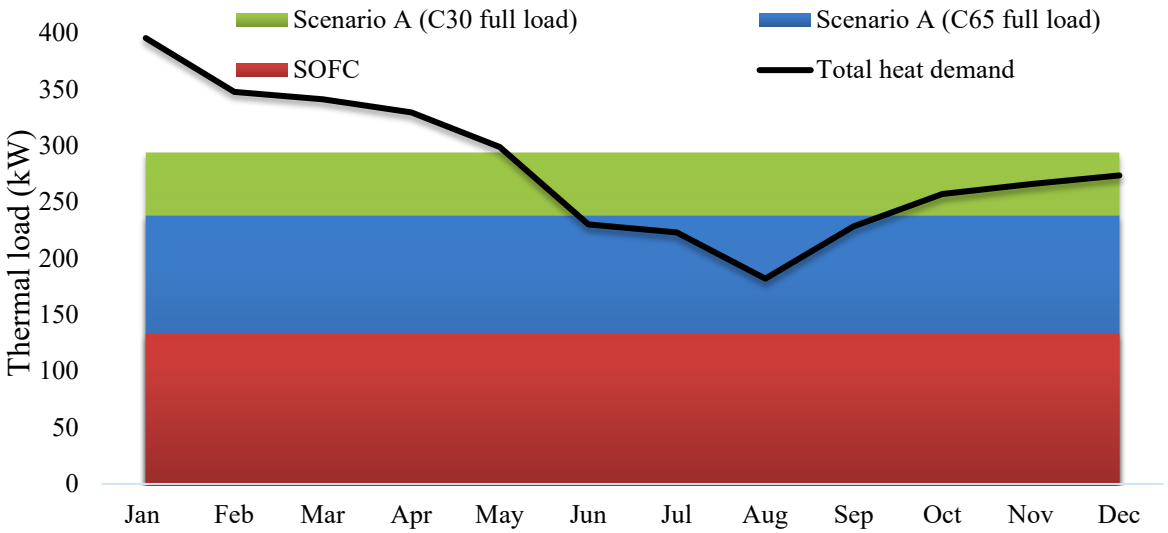

b)

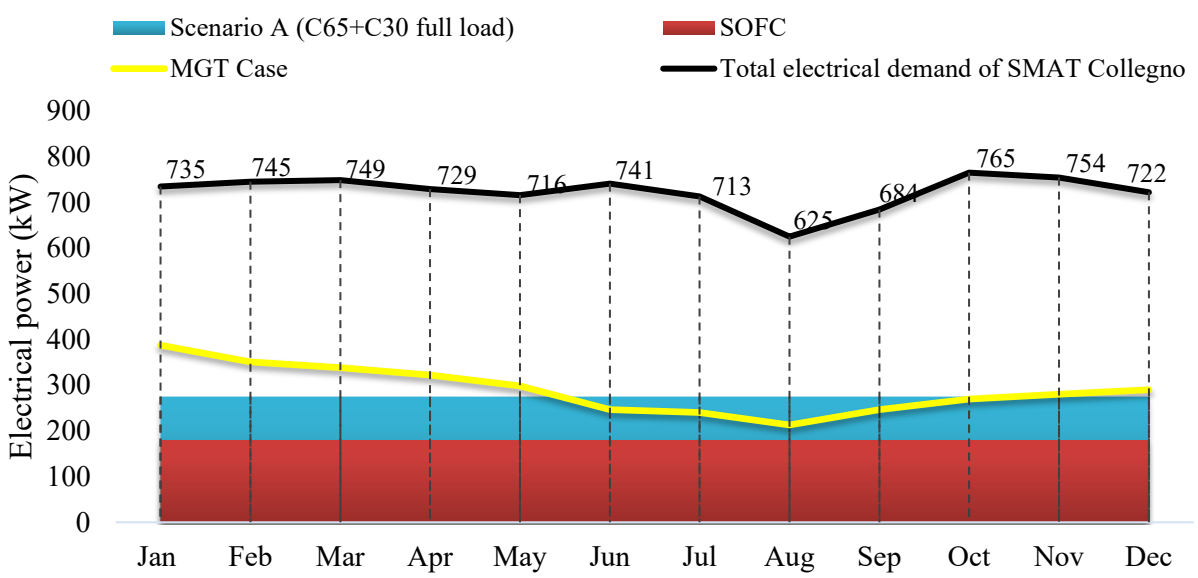

c)

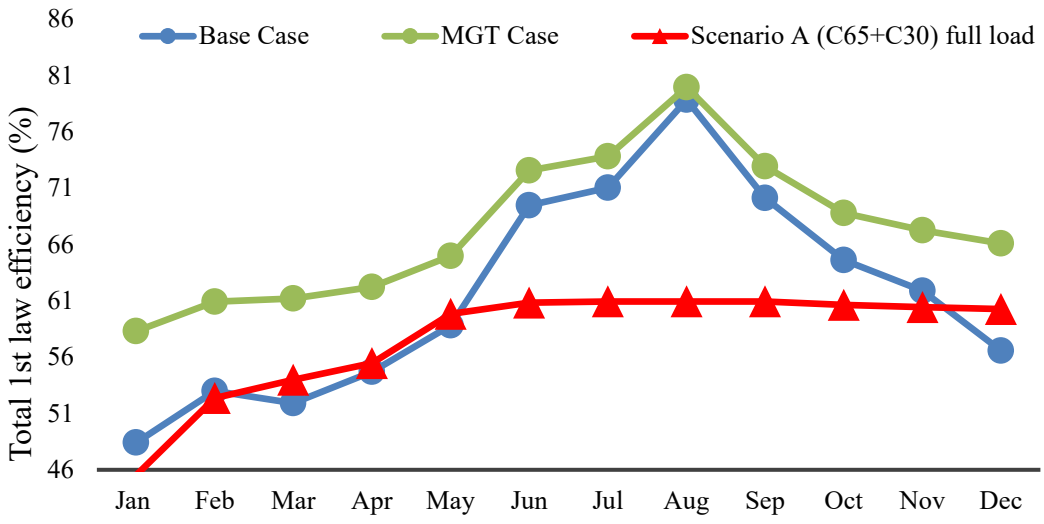

Figure 24. a) Thermal load, b) Electrical power and c) Total efficiency for Scenario A.

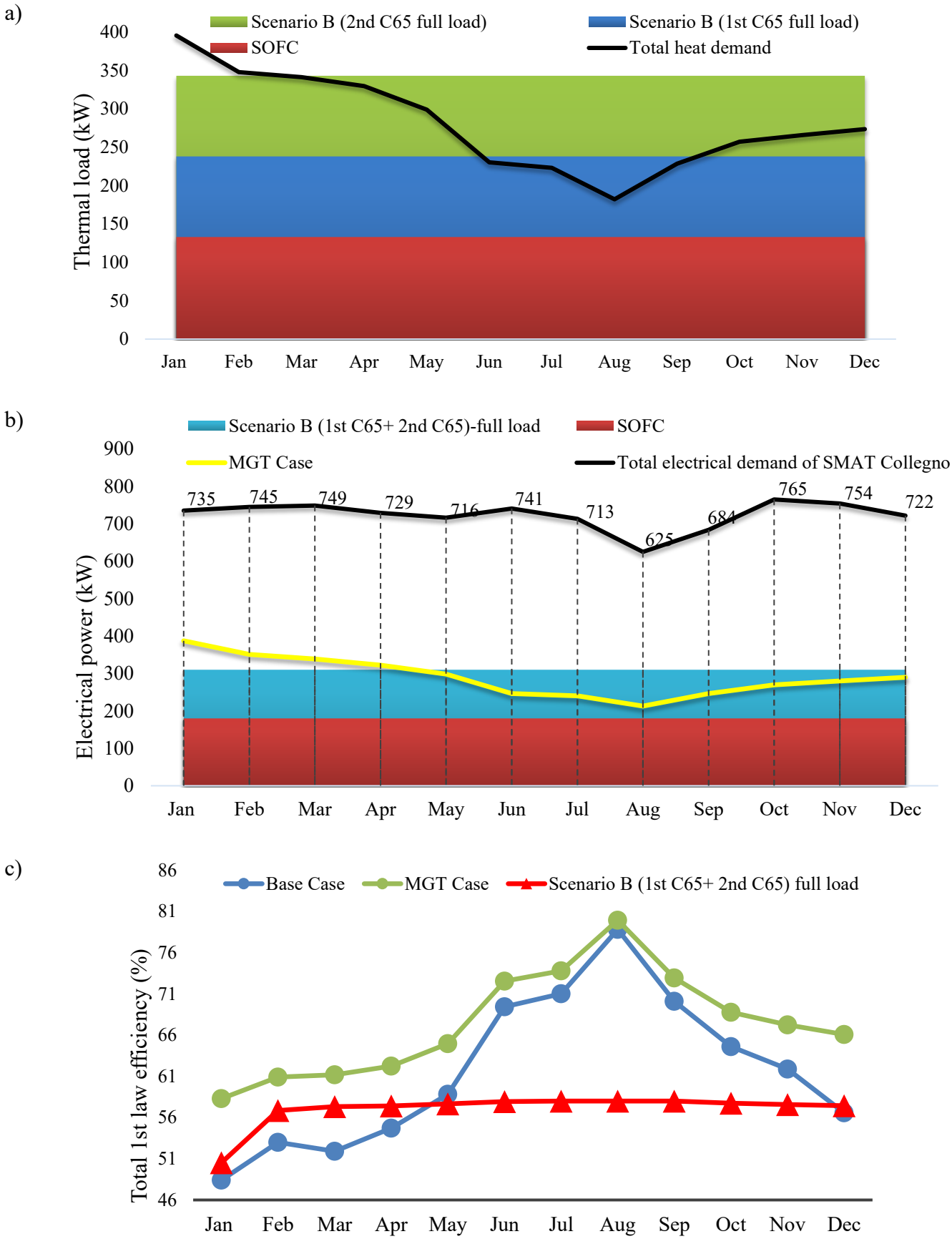

Figure 25. a) Thermal load, b) Electrical power and c) Total system efficiency for Scenario B

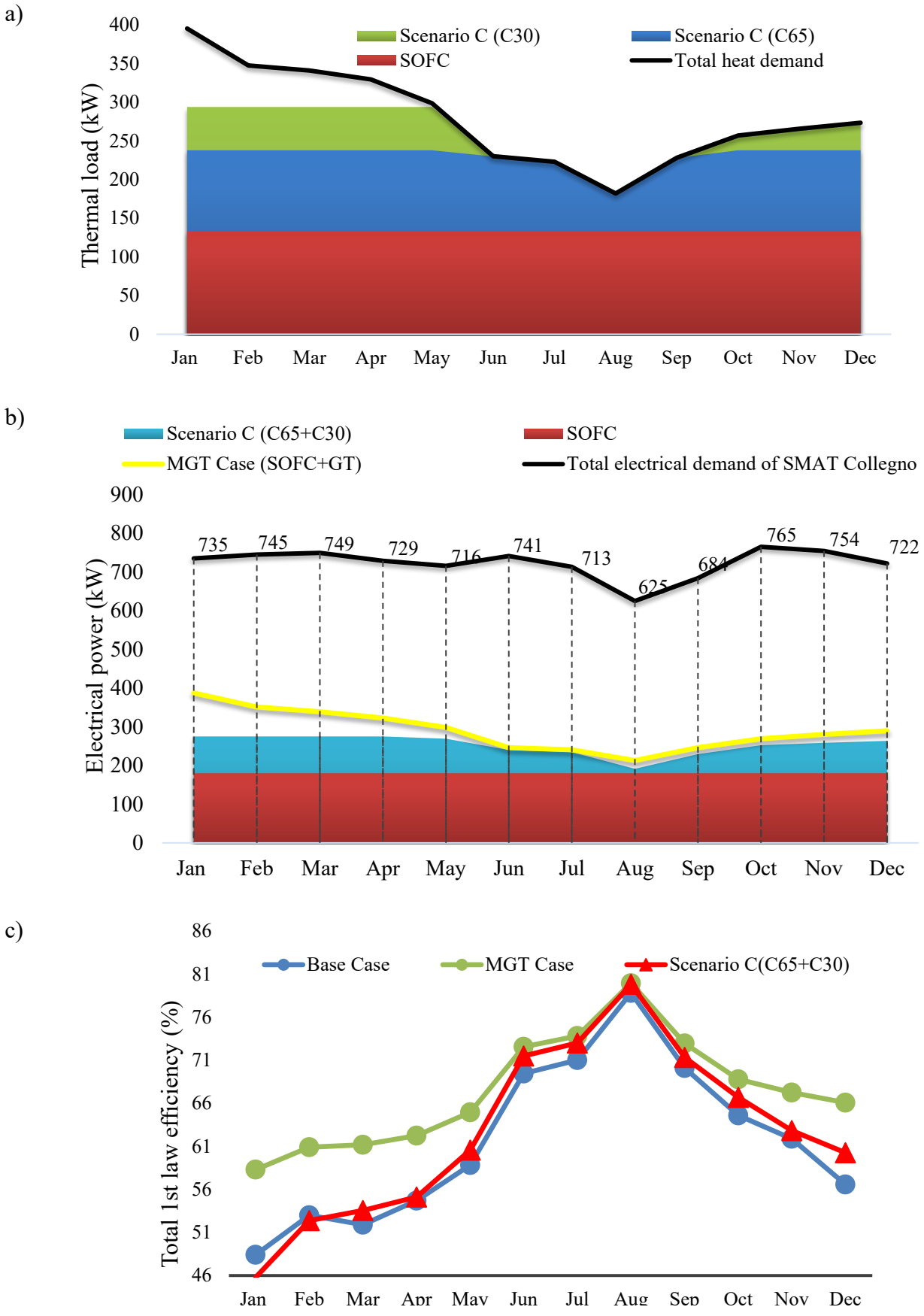

Figure 26. a) Thermal load, b) Electrical power and c) Total system efficiency for Scenario C

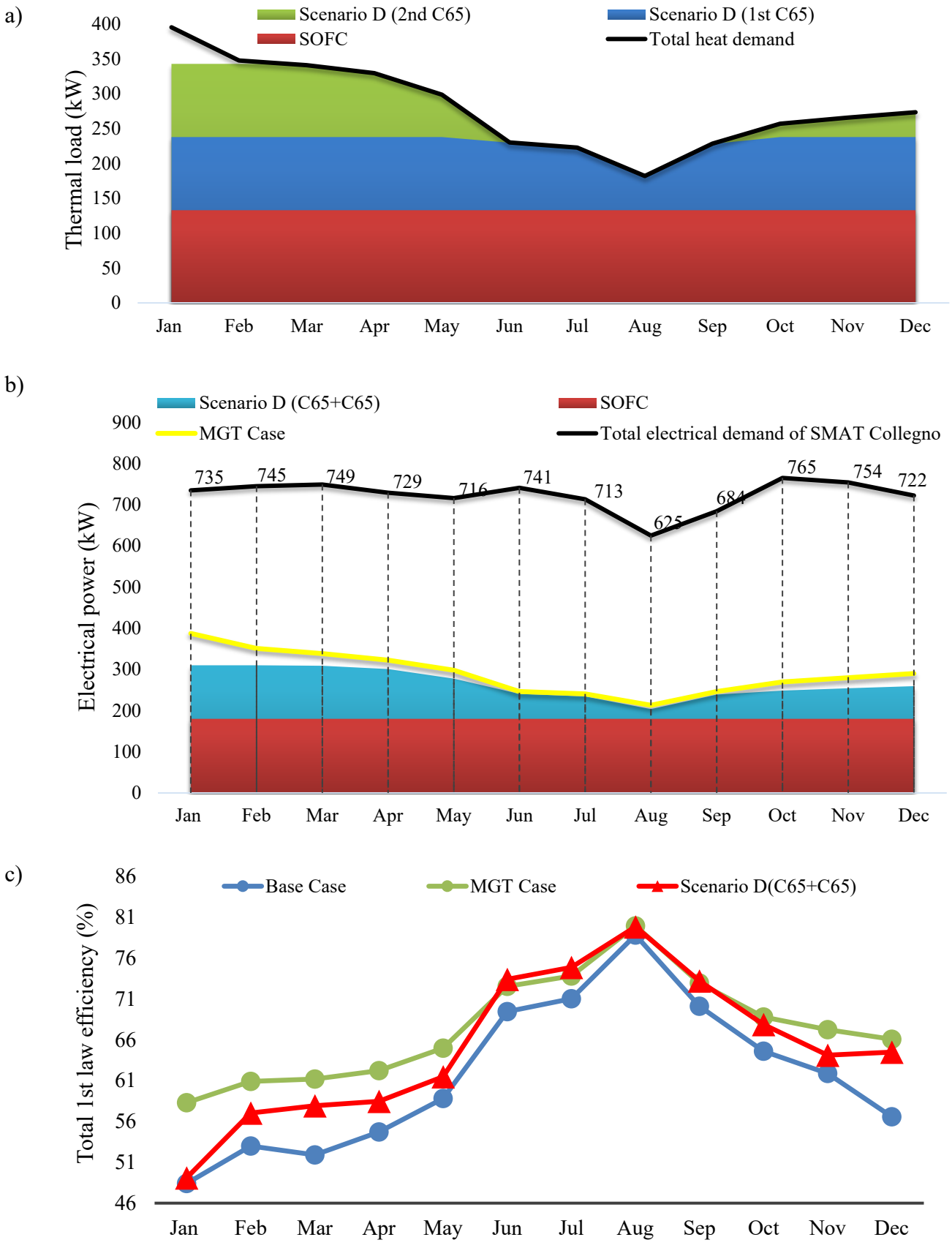

Figure 27. a) Thermal load, b) Electrical power and c) Total system efficiency for Scenario D

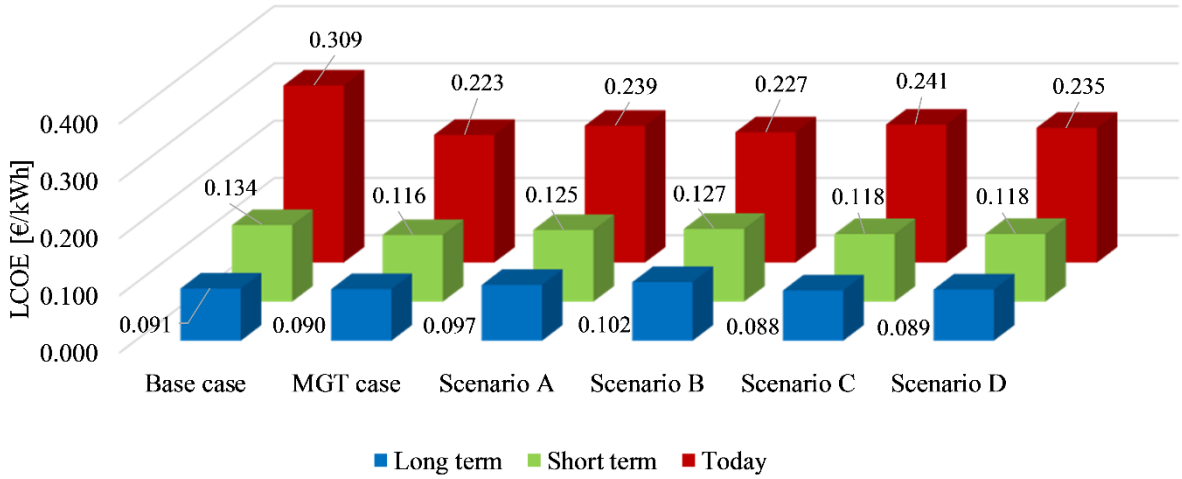

Figure 28. Levelized cost of electricity for the different scenarios and cost trajectories.

940

941 **Tables' caption**

952

953

954

955

956

957

958

959

960

961

962

963

964

965

966

967

968

969

970

971 **Tables**

972 Table 10. Material Resistivity used for Ohmic voltage loss estimation [21]

Component	Material	Resistivity	Thickness (mm)
Anode	Ni/YSZ cermet	$\rho_{an}=2.98\times10^{-5}\exp(\frac{-1392}{T_{FC,e}})$	0.5
Cathode	LSM-YSZ	$\rho_{cat}=8.114\exp(\frac{600}{T_{FC,e}})$	0.05
Electrolyte	YSZ	$\rho_{ely}=2.94\times10^{-5}\exp(\frac{10350}{T_{FC,e}})$	0.01
Interconnection	Doped LaCrO3	0.0003215	-

973

974

975 Table 11. Parameters correspond to the material anode and cathode sides [21]

Component	Parameter	Value	Unit
Anode	Pre-exponential factor for anode, γ_{an}	6.54×1011	A m-2
	Activation energy for anode, $E_{a,an}$	140,000	J mol-1
Cathode	Pre-exponential factor for cathode, γ_{ca}	2.35×1011	A m-2
	Activation energy for cathode, $E_{a,cat}$	137,000	J mol-1

976

977 Table 12. Main parameters for digester thermal load calculations.

Parameter	Symbol	Value	Unit	Ref.
Sludge inlet temperature	$T_{sl,in}$	14 (January) ÷ 23 (July)	°C	[29]
Sludge mass flow rate	$\dot{m}_{sl}$	1.82 (December) ÷ 3.09 (May)	kg/s	SMAT
Heat transfer coefficient for underground walls	U_{ug}	2.326	W/m²°C	SMAT
Heat transfer coefficient for non-underground walls	U_{ext}	0.930	W/m²°C	SMAT
Area of underground walls (floor and partial side walls)	A_{ug}	450.8	m²	SMAT
Area of non-underground walls (partial side walls and roof)	A_{ext}	1132.1	m²	SMAT
Ground temperature	T_{gr}	5 (winter) ÷ 10 (summer)	°C	Assumption
External temperature	T_{ext}	2.3 (February) ÷ 23.9 (July)	°C	ilmeteo.it
Percentage of losses through pipes	$\%_{pipes}$	5	%	Assumption

Table 13. Comparison of results obtained from the present work with the experimental values reported by Tao et al. [22]

Current density (A/m^2)	Cell voltage (V) (Present work)	Cell voltage (V) (Tao et al.)	*Error (%)*	Power density (W/m^2) (Present work)	Power density (W/m^2) (Tao et al.)	*Error (%)*
2000	0.742	0.76	-1.368	0.148	0.15	-1.333
3000	0.684	0.68	0.272	0.205	0.21	-2.381
4000	0.634	0.62	0.868	0.253	0.26	-2.692
5000	0.582	0.57	0.684	0.294	0.295	-0.339
6000	0.547	0.52	1.404	0.328	0.315	4.127

Table 14. SOFC, biogas processing unit and MGT costs. [23] [24] [25]

	Today	**Short Term**	**Long term**
Units manufactured	-	500	5,000
Module CAPEX (€/kWe)	17,908	5,656	2,326
Maintenance (€/kWe/yr)	120	60	47
Stack replacement (€/kWe)	2,710	712	482
Stack lifetime during 15 years (y)	3-3-4-4	5-5-5	7-8
Clean-up system CAPEX (€/kWe)	1,500	1,000	500
Clean-up system OPEX (c€/kWhe)	1	1	0.5
MGT CAPEX (€/kWe)	1,000	1,000	1,000
MGT OPEX (c€/kWhe)	1	1	1

Table 15. Matrix of the analyzed case studies.

		SOFC and Clean-up costs		
		Present	Short term	Long Term
Plant lavout	***Base Case***	***Base 1***	***Base 2***	***Base 3***
	MGT case	MGT1	MGT2	MGT3
	Scenario A	A1	A2	A3
	Scenario B	B1	B2	B3
	Scenario C	C1	C2	C3
	Scenario D	D1	D2	D3

Table 16. Configurations and operating conditions of the investigated scenarios.

Scenario	Module	Load
Scenario A	SOFC C65 C30	Full load Full load Full load
Scenario B	SOFC C65 C65	Full load Full load Full load
Scenario C	SOFC C65 C30	Full load Full/Partial load Full/Partial load
Scenario D	SOFC C65 C65	Full load Full/Partial load Full/Partial load

Table 17. LCOE and PBT for the different technical scenario, with a short term economic scenario.

Scenario	LCOE (€/kWh)	CAPEX share of LCOE (€/kWh)	OPEX share of LCOE (€/kWh)	PBT (y)
Base Case	0.134	0.057	0.076	11.57
MGT Case	0.116	0.042	0.075	7.66
Scenario A	0.125	0.040	0.085	8.46
Scenario B	0.127	0.037	0.090	8.30
Scenario C	0.118	0.044	0.074	8.01
Scenario D	0.118	0.043	0.075	7.95

Table 18. Electrical and natural gas yearly consumption for the different scenarios.

	SOFC size [kW]	MGT size [kW]	Yearly NG to MGT (Nm^3)	Yearly biogas to boiler (Nm^3)	Yearly NG to SOFC (Nm^3)	Yearly NG to boiler (Nm^3)	Total yearly NG consumption (Nm^3)	Total yearly electricity production (kWh)
Base case	180	0	0	165,411	11,630	33,718	45,348	1,576,800
MGT Case	180	210	134,405	173,153	11,630	0	146,036	2,539,854
Scenario A	180	95	162,740	173,153	11,630	19,528	193,898	2,409,000
Scenario B	180	130	242,928	173,153	11,630	4,584	259,141	2,715,600
Scenario C	180	95	87,028	173,153	11,630	19,528	118,186	2,217,000
Scenario D	180	130	116,243	173,153	11,630	4,584	132,458	2,324,141